

#### **Dinis Granadeiro Pires Madeira**

Licenciatura em Engenharia Química

## Development of a toolbox for *in silico* experiment free culture media design based on *prior* metabolic knowledge

Dissertação para obtenção do Grau de Mestre em Engenharia Química e Bioquímica

Orientador: Rui Oliveira, Professor Associado , FCT-UNL

Co-orientador: Rafael S. Costa, Doutor, FCT-UNL

Júri:

Presidente: Professor Doutor Mário Fernando José Eusébio

Arguentes: Professor Doutor Ludwig Krippahl

Vogais: Professor Doutor Rui Manuel Freitas Oliveira

Março, 2020



elopment of a tooll abolic knowledge	box for <i>In</i>	silico expo	eriment	t free	cultur	e media	design	based on <i>prior</i>	r
: 1, 0 D: : C	1 · D:	37.1.	г 1		G:A			•	

Copyright © Dinis Granadeiro Pires Madeira, Faculdade de Ciências e Tecnologia, Universidade Nova de Lisboa.

A Faculdade de Ciências e Tecnologia e a Universidade Nova de Lisboa têm o direito, perpétuo e sem limites geográficos, de arquivar e publicar esta dissertação através de exemplares impressos reproduzidos em papel ou de forma digital, ou por qualquer outro meio conhecido ou que venha a ser inventado, e de a divulgar através de repositórios científicos e de admitir a sua cópia e distribuição com objetivos educacionais ou de investigação, não comerciais, desde que seja dado crédito ao autor e editor.

### Resumo

O desenho de meios de cultura desempenha um papel vital na performance dos meios de cultura nomeadamente na concentração celular, viabilidade das células, rendimento e qualidade de produto produzido. O principal objetivo da presente dissertação é desenvolver um método computacional em MATLAB para o design de meios de cultura in silico com base em conhecimento metabólico prévio, sem a necessidade de experiências laboratoriais. Foi usado como caso de estudo uma rede metabólica para as células de ovário do hamster chinês (CHO), as células CHO são atualmente as principais células de mamífero utilizadas na produção de proteínas recombinantes para uso na indústria farmacêutica e aplicações terapêuticas. A técnica da análise dos modos elementares foi usada para calcular o número total de elementary modes (EM) da rede metabólica CHO, estes são usados para calcular a footprint (pegada) dos metabolitos extracelulares no meio de cultura para os diferentes metabolismos celulares. O conjunto de todas as footprints da rede metabólica foi nomeado de footprintome. O método "Pattern clustring" foi utilizado para reduzir o footprintome. Duas footprints foram calculadas para representar a totalidade do footprintome, usando dois métodos de cálculo, a média aritmética de todas as footprints presentes no footprintome e a média ponderada pela energia livre de Gibbs. Comparouse os resultados obtidos com dados da literatura e observou-se que 21 dos 26 metabolitos extracelulares presentes nos dados da literatura estão dentro do intervalo de variância dos resultados obtidos. Também foi desenvolvido um método para calcular meios de cultura específicos baseados no fenótipo de cada footprint, duas fórmulas de meios de cultura foram calculadas uma para crescimento celular e outra para produção de imunoglobulina G (IgG), a fórmula para crescimento celular foi comparada com uma fórrmula de meio de cultura CHO testada em laboratório, concluindo-se que esta ferramenta computacional é capaz de calcular fórmulas de meios de cultura, que posteriormente podem ser testadas em laboratório.

**Palavras Chave:** desenho de meios de cultura, *análise dos modos elementares*, redes metabólicas, Chinese Hamster Ovary (CHO)

## **Abstract**

Culture media design plays a vital role in culture performance, namely cell density, cell viability, product yield and product quality. The main goal of the present M.Sc. thesis is to develop a method for in silico culture media design based on prior metabolic knowledge of the targeted cell line, reducing the burden of laboratory experiments. A Chinese Hamster Ovary (CHO) cell line was used as case study. CHO cells are the main mammalian host used today in the biopharmaceutical industry for the production of recombinant proteins for therapeutics and pharmaceutical applications. Elementary mode analysis (EMA) was applied to compute the total number of elementary modes (EM) of a representative CHO metabolic network. From the full set of EMs, the extracellular metabolite footprints for different metabolic states were computed. The full set of metabolic footprints was named footprintome. Footprintome reduction was achieved by pattern clustering. Two footprints were computed representing all of the Footprintome by averaging based on number and averaging based on Gibbs free energy. These footprints were compared with literature data resulting in significant similarities. More specifically, 21 out of the 26 extracellular metabolites present in the literature data are within the variance intervals of the computed footprintome. Afterwards a phenotype-targeted design was applied to compute custom culture media formulas for cell growth and for Immunoglobulin G (IgG) production. The cell growth formula was compared with a lab tested CHO culture medium formula, showing that this tool is capable of computing culture media formulas that can be further tested in the lab.

**Keywords:** culture media design methods, elementary mode analysis, metabolic networks, Chinese Hamster Ovary (CHO)

## Index

Abstract	V
Figure Index	VIII
1. Introduction	1
1.1 Culture Media Design Methods	3
1.1.1 Plackett and Burman design	5
1.1.2 Taguchi design	6
1.1.3 Response Surface Methodology	7
1.1.4 Artificial neural network	8
1.1.5 Genetic Algorithm	10
1.2 Metabolic modelling methods	12
1.2.1 Metabolic flux analysis (MFA)	13
1.2.2 Flux balance analysis (FBA)	14
1.2.3 Elementary mode analysis	15
1.4 M.Sc. thesis objectives	17
2.4.1 Calculation of elementary mode Gibbs free energy of reaction ( $\Delta G^{o}r$ )	21
2.4.2 Clustering based on phenotype similarity	22
3. Results and discussion	25
3.1 Chinese Hamster Ovary Cells (CHO) metabolic network	25
3.2 Computation of CHO Elementary Modes	26
3.3 Computation and reduction of CHO footprintome	29
3.4. Comparison with experimental data	33
3.4. Phenotype-targeted culture media design	36
3.4.1 Minimization of lactate and ammonium buildup	37
3.4.2 Minimization of osmolarity buildup	39
3.4.3 Final culture media concentrations	41
4. Conclusions	44
5. References	46
Appendix	53
Appendix A – CHO Metabolic Networks	53
Appendix C - Standard Gibbs free energy of formation of metabolites values	66
Appendix D - Literature data cell growth rate and metabolic rates 62	67
Appendix E - Arithmetic footprint and computed formulas for Biomass and IgG pronetworks	ducing

 $Appendix \ F-Results \ from \ the \ IgG \ producing \ network \ \textit{footprintome} \ automatic \ reduction... \ 70$ 

## Figure Index

Figure 1 - Culture media design methodologies	.3
Figure 2 - Response surface for an exemplary model	.7
Figure 3 - Multi layered perceptron neural network	.9
Figure 4 - GA basic flow scheme	.10
Figure 5 - Example of culture media optimization using GA	.11
Figure 6 - Example of a simple metabolic Network	12
Figure 7 - FBA example, restrictions and objective function	14
Figure 8 - Elementary modes of the Fig. 6 network	.15
Figure 9 - Admissible Flux Space of the Fig. 6 network elementary modes	15
Figure 10 - Example of a Chinese Hamster Ovary Cell elementary mode	.18
Figure 11 - Reduced <i>footprintome</i> for biomass production after 2 steps of reduction: Step 1-	
biomass production, Step 2-Thermodynamic reduction	.31
Figure 12 - Reduced <i>footprintome</i> for biomass production after 3 steps of reduction: Step 1-	
biomass production, Step 2-Thermodynamic reduction, Step 3- Pattern clustering with	
· · · · · · · · · · · · · · · · · · ·	.32
Figure 13 - Comparison between theoretical footprints computed by the arithmetic average	
method and the weighted average method with experimental footprint	34
Figure 14 - Histogram $\Delta G^0_r$ of each EM for the biomass producing network	.36
Figure 15 - Reduced <i>footprintome</i> for biomass production after 4 steps of reduction: Step 1-	
biomass production, Step 2-Thermodynamic reduction, Step 3- Pattern clustering with	
arithmetic averaging, Step 4- Elimination of all footprints that either produce lactate or	
ammonium.	.38
Figure 16 - Comparison between the optimal EM computed for the biomass producing netwo	
and the respective arithmetic footprint	
Figure 17 - Comparison between the optimal EM computed for the IgG producing network an	ıd
the respective arithmetic footprint	.41
Figure 18 - Comparison between the computed formula for biomass synthesis with CHO	
culture media	.42

## Table Index

Table 1 Culture media design studies over the years	13
Table 2 Plackett and Burman design of experiments	14
Table 3 Taguchi Signal -to -Noise Ratios.	15
Table 4 Elementary mode count of the biomass and product producing networks	37
Table 5 Footprint of the EM represented in Appendix B, Table B.1	39
Table 6. Automatic <i>footprintome</i> reduction results	40
Table 7 MSE between measured and theoretical footprint	46
Table 8 Computed formulas for IgG and biomass syntheses and Lab tested CHO culture media.	54

## 1. Introduction

The optimisation of the composition of culture media has been historically a very important factor for the performance of cell culture. Historically the main drivers have been the maximization of cell density, cell viability, product titer and product yield. In many cases the positive impact of culture media surpasses that of genetic engineering. The creation and optimization of culture media that supports the growth of microorganisms or cells comes with a set of challenges, particularly, the creation of methods that can achieve the best results, while being time and cost effective. There are several methodologies in use today, in this introduction we will be giving a brief history and definition about the different methods for culture media design. A more detail explanation about this methods, their advantages and disadvantages will be discussed in further chapters of this work.

Culture media design started with classical methods using one-factor-at-time experiments which consists in changing one factor for each experiment until we have a desired result. This method was primarily used in culture media design until the mid-twenties century, when it was replaced by design of experiments methods (DoE). One of the early forms of this was the Plackett and Burman design (PBD) created by Plackett R. L. and Burman J. P. in 1946, it is a two level design method used to detect the top contributing factor, assuming that the interaction between two or more factors are negligible, PBD is still in use today, primarily for the elimination of noncontributing factors (screening) in the early stages of culture media design.

A few years later the Central Composite Design (CCD) DoE was created by Box G. E. P. and Wilson K. B.<sup>2</sup> in 1951 to overcome some of the limitations of PBD. The CCD is composed by 3 sets of points: a factorial set, each having two levels, a center set, whose values are the median values of each factor, and an axial set that are identical to the center points except for one factor. Today this design is mainly used in the Response Surface Methodology (RSM) also developed by Box G. E. P. and Wilson K. B.<sup>2</sup>, a DoE is ran and then RSM is used to create a mathematical model that uses statistical design of experiments and regression analysis to obtain the best formulations This method is still to date, the most used method in the industry to optimise culture media.

The Taguchi method was created by Genichi Taguchi <sup>3</sup> in 1992, this method is based on noise analysis (uncontrollable variables in the experiments), making it a useful method for measuring the characteristics deviation of the target value. Taguchi method uses an orthogonal array of experiments and unlike PBD, it analyses the main effect and two factor iterations.

The artificial neural networks (ANN) are a computing system inspired by the neural connections in the animal brains, the first computational model was created by Warren M. and Walter P.<sup>4</sup> in 1943, the technology continued to advance through the century and the first application of ANN in culture media design was the work done by Glassey J et. al.<sup>5</sup> in a Escherichia coli *batch* fermentation in 1994. ANN can process a large amount of information, which is useful in culture media design, that often contains hidden patterns and large amounts of variables.

A genetic algorithm (GA) mimics the process of natural selection by relying on biologically inspired operators such as mutation, crossover and selection<sup>6</sup>. These types of algorithms started to be applied in culture media design in the 1990s. One of the first examples of this approach used in culture media design was the work proposed by Weuster-Botz D and Wandrey<sup>7</sup>, with the optimization of a culture media for a *Candida boidinii* fermentation.

In this work will also be discussed different analysis tools to determine metabolic fluxes in metabolic networks. These types of analysis are the basis for metabolic engineering which is defined as the "direct improvement of product formation or cellular properties through the modification of specific biochemical reactions or introduction of new ones with the use of recombinant DNA technology", as such metabolic engineering uses metabolic networks to determine metabolic fluxes that characterize cell physiology and control cell metabolism<sup>8</sup>. The analysis of a metabolic networks is based on the principle of mass conservation of internal metabolites within a system<sup>9</sup>. Depending on what type of analysis we want, there are three main techniques: metabolic flux analysis(MFA)<sup>10</sup>, flux balance analysis (FBA)<sup>11</sup> and elementary mode analysis (EMA)<sup>12</sup>. These techniques and how they can be applied in culture media design will be explain in more detail in the next chapters of this work.

#### 1.1 Culture Media Design Methods

Culture media design methods can be classified as (Fig. 1):

- Traditional one-factor-at-a-time
- Advanced statistical/mathematical methods (the most frequently applied today)
- Advanced system biology methods

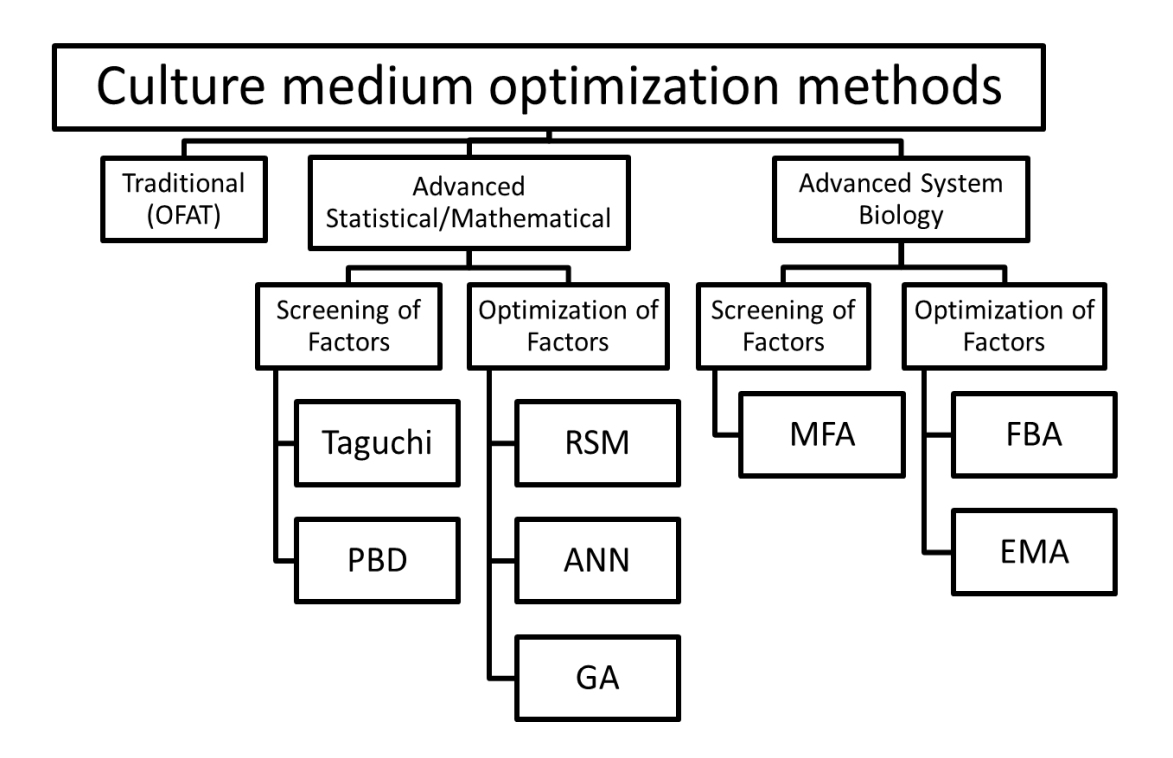


Figure 1 - Culture media design methodologies . PBD: Plackett and Burman Design; RSM: Response Surface Method; (Adapted from: Singh V, Haque S, Niwas R, Srivastava A, Pasupuleti M and Tripathi C K M 2017 Strategies for fermentation media optimization: An in-depth review Front. Microbiol. **7**85)

In this context, it is important to distinguish two different problems: screening and optimization of factors. Screening of factors is typically the first step in a culture media design project. It aims to identify the principal contributing factors that should be optimized in the proceeding steps. Optimization of factors aims at optimizing the media components quantities (typically concentrations) to enforce maximal product synthesis and/or maximal cell growth while minimizing unwanted by-products, such as lactate and ammonia. Table 1 overviews some of the published studies for culture media design methods.

 $\ \, \textbf{Table 1 - Culture media design studies over the years} \,$ 

Screening method / DOE	Optimization method	Experiments	Number of Factors	Metabolite	Cell line	Optimization	Year	Reference
Taguchi	-	16	4	hyaluronic acid	Streptococcus sp.	112%	2009	13
Taguchi	-	9	4	N-acetylchitooligosaccharide	Streptomyces chilikensis	126,86%	2019	14
Taguchi	-	16	4	Bioethanol	Saccharomyces cerevisiae	37,50%	2019	15
Taguchi	-	8	6	Mixed alcohols	Clostridium pasteurianum	78,48%	2013	16
Taguchi	-	18	8	Amidase	Geobacillus subterraneus	113,79%	2016	17
PBD	-	16	12	Lipase	Candida rugosa	-	2008	18
Taguchi - CCD	RSM	12 - 27	10-4	Vanillin	Psychrobacter sp.	-	2012	19
Taguchi - CCD	RSM	18 -27	8-4	Lipase	Rhizopus chinensis	120%	2008	20
CCD	RSM	20	3	b-carotene	Daucus carota	141,33%	2008	21
CCD	RSM	50	5	Lipase	Aryabhattai SE3-PB	618,45%	2018	22
CCD	RSM	17	3	Y-aminobutyric acid	Streptococcus thermophilus	20%	2018	23
PBD - CCD	RSM	20- 32	12-5	Glycolipopeptide Biosurfactant	Pseudomonas aeruginosa	-	2017	24
PBD - CCD	RSM	8 - 13	5-2	Exopolysaccharides	Cordyceps militaris	96,00%	2010	25
-	GA	80	11	-	Helicoverpa zea (insect cell)	550,00%	2002	26
-	GA	98	14	2-Phenylethanol	Kluyveromyces marxianus	32,00%	2004	27
-	GA	270	12	Eicosapentaenoic acid	Nannochloropsis gaditana	23,00%	20015	28
-	GA	544	26	yessotoxins	Dinoflagellates	60,00%	2011	29
CCD	ANN	20	3	avermectin B1b	Streptomyces avermitilis	50,78%	2014	30
CCD	ANN-GA	ANN-GA 36		Cholesterol Oxidase	Streptomyces Sp.	132,14%	2015	31
	RSM-GA		5			49,60%		
CCD	ANN-GA	20		Lipase	Soil Microorganism (Not Specified)	19,41%	2007	32
	RSM-GA		3			10,56%		

(Experiments and number of factors are represented for screen method and Doe method respectively in cases were both take part in the study).

#### 1.1.1 Plackett and Burman design

The PBD method focuses on the main effect of each factor, assuming that, interactions of two or more factors are negligible, it is used for factor screening in the beginning of a culture media design process. PBD is a two-level factor design, a high level (+) and a low level (-), there are two types of variables: "real variables", who's values changes during experiments, and "dummy variables", whose values remain the same. Classical experiments before the execution of the PBD helps in the selection of independent and dummy variables. Table 2 represents a Plackett and Burman design of experiments for 12 runs and 11 two-level factors, usually in culture media design, factors values represent concentration values of different compounds in the media.

Table 2 - Plackett and Burman design of experiments

						<b>FACT</b> (	ORS				
RUN	X1	X2	X3	X4	X5	X6	X7	X8	X9	X10	X11
1	+	+	+	+	+	+	+	+	+	+	+
2	_	+	_	+	+	+	_	_	_	+	_
3	_	_	+	_	+	+	+	_	_	_	+
4	+	_	_	+	_	+	+	+	_	_	_
5	_	+	_	_	+	_	+	+	+	_	_
6	_	_	+	_	_	+	_	+	+	+	_
7	_	_	_	+	_	_	+	_	+	+	+
8	+	_	_	_	+	_	_	+	_	+	+
9	+	+	_	_	_	+	_	_	+	_	+
10	+	+	+	_	_	_	+	_	_	+	_
11	_	+	+	+	_	_	_	+	_	_	+
12	+	_	+	+	+	_	_	_	+	-	_

The effect of each factor is given by Eq. 1:

$$Eff = 2 * \left(\sum Yh - \sum Yl\right)/N\right) \tag{1}$$

Where Eff is the effect of a factor (objective function), Yh is the value given for the high level experiments, Yl is the value given for the low level experiments and N is the total number of runs.

The experimental error is calculated by using the effects of the "dummy variables" (Eq. 2).

$$Veff = \sum \frac{Ed^2}{n}$$
 (2)

Where Veff is the variance of the effect Ed, Ed is the effect of a "dummy variable" and n is the number of "dummy variables".

The standard error is the square root of the variance Veff and the significant level of the effect of each variable is determined by a t-test distribution and the variables with a confidence level greater than 90% or 95% are chosen.

Examples of culture media design utilizing PBD are the statistical evaluation of a culture media components for lipase production by Pseudomonos fluorescens made by Rajendran A. et. al. 18 and the screening of components for protease production by *Bacillus safensis* in a submerged fermentation <sup>33</sup>.

Its main advantages are the screening of high number of factors using a low number of experiments, capable of screening n factors in n + 1 experiments, saving both time and money at the cost of neglecting two factor interaction, remaining a simple and practical screening method to use in the initial stages of culture media design.

#### 1.1.2 Taguchi design

Taguchi method is based in an orthogonal array of experiments. Taking focal point in noise factor analysis (uncontrollable factors that affect the result of experiments and generally cause loss of quality), through the use of a signal-to-noise ratio (S/N), Taguchi methodology can be used in the initial stages of culture media design to identify which factors are more influential.

First we identify the control factors (controllable factors), their levels and the appropriate orthogonal array (based on the degrees of freedom), once we got the measured experiment values, we calculate the (S/N) ration for each experiment. There are three signal-to-noise ratios: smaller the better, larger the better and nominal the best. Table 3 describes these three ratios.

Table 3 - Taguchi Signal -to -Noise Ratios

Smaller the better 
$$\left(\frac{S}{N}\right) = -10 * log 10 \left[\left(\frac{1}{n}\right) * \sum_{i=1}^{n} Yi^{2}\right]$$
 (3)

Larger the better  $\left(\frac{S}{N}\right) = -10 * log 10 \left[\left(\frac{1}{n}\right) * \sum_{i=1}^{n} \frac{1}{Yi^{2}}\right]$  (4)

Nominal the best  $\left(\frac{S}{N}\right) = 10 * log 10 \left(\frac{Mean^{2}}{Variance}\right)$  (5)

Larger the better 
$$\left(\frac{S}{N}\right) = -10 * log 10 \left[\left(\frac{1}{n}\right) * \sum_{i=1}^{n} \frac{1}{Yi^2}\right]$$
 (4)

Nominal the best 
$$\left(\frac{S}{N}\right) = 10 * log 10 \left(\frac{Mean^2}{Variance}\right)$$
 (5)

Where Y is the experiment result, n is the total number of experiments and for the nominal the best S/N ratio, the Mean and Variance are for a chosen set value.

Next, we calculate the S/N value for each level of the control factors. Eq. 6 shows the S/N values for the control factor {i} level {j}.

$$\frac{S}{N}ij = \sum_{k}^{n} \frac{S}{N}k \tag{6}$$

With n being the total number of experiments with the factor  $\{i\}$  on level  $\{j\}$ .

The S/N values for the different levels of a factor are compared between each other and those with the highest value are chosen, being the levels that minimize the effect of noise. With Taguchi method we can chose the set of control factors levels that minimizes the effect of noise for the objective function in study.

An example of culture media design study using Taguchi method is the work done by Makowski K. et. al<sup>34</sup>. It comprises the optimization of a culture media, for the production of microorganisms active in odorous compound removal. Another example is the optimization of media component for the production of N-acetylchitooligosaccharide from chitin by *Streptomyces chilikensis* <sup>14</sup>.

Contrary to PBD method, the Taguchi is a more complex and complete approach, that can detect 2 factors interaction but is still far away of describing a whole microorganism metabolism.

#### 1.1.3 Response Surface Methodology

Response surface methodology (RSM) it's a complex mathematical method for the optimization of culture media design, which includes statistical experimental design and regression analysis<sup>2</sup>. It is used after the implementation of a PBD or CCD design of experiments. RSM optimization includes three main steps, experimental design (screening of factors), the path of steepest ascent/descent and the quadratic regression mode.

After identifying the main effects, the next step is to explore the region of the operation conditions. This region is called the *response surface* (Fig. 2) and the goal is to conduct a series of experiments to find the path of the steepest ascend or descend given by the initial set of experiences <sup>35</sup>. A first order model can be used (Eq. 7), containing only the main effects and its interactions.

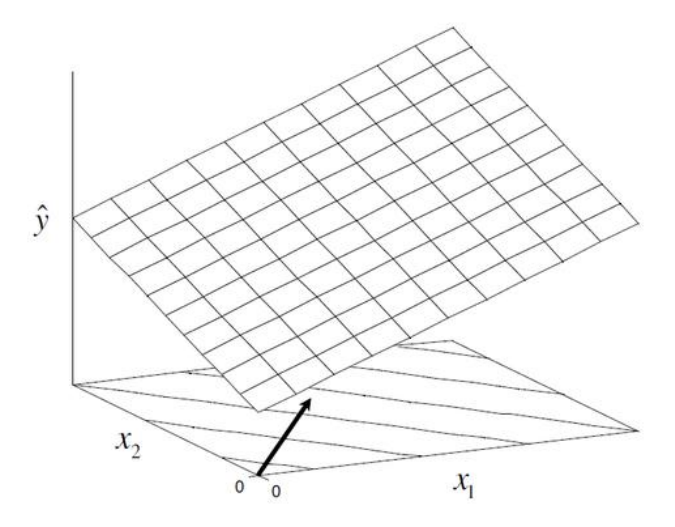


Figure 2 - Response surface for an exemplary model

$$Y = a_0 + a_1 x_1 + a_2 x_2 + a_{12} x_1 x_2 + e \tag{7}$$

Where Y is the predicted response, e represents the effects of uncontrollable variables (noise) and  $a_i$  the regression coefficients of a factor i.

In RSM, when close to the optimum region, in which a first order model is no longer adequate, it is also applied a second order model. The second order regression model is presented in Eq. 8:

$$Y = a0 + \sum_{i=0}^{N} aiXi + \sum_{i< j}^{N} aijXiXj + \sum_{i=0}^{N} aiiXi^{2}$$
 (8)

Where  $a_iX_i$  are the linear terms,  $a_{ij}X_iX_j$  are the interaction terms and  $a_{ii}X^2$  are the square terms.

The main advantage of using RSM is the ability to study the effects of the factors in the response throughout the entire surface region, capable of predicting an optimum response. Examples of culture media design using RSM are the culture media optimization for  $\beta$ -carotene and biomass production in *Dunaliella salina* in mixotrophic culture<sup>36</sup>, and the optimization of lipase production in *Bacillus aryabhattai* ( $^{22}$ ).

However, the RSM also has its limitations, the complexity of microorganism metabolism, its nonlinear nature and the low availability of quality kinetic data<sup>37</sup>, makes the modeling of biological reaction systems a challenge. Also it is difficult to study interaction of five or more factors, this is a problem because culture media can have up to 100 different components, this coupled with the fact that the experiment numbers needed to optimize 100 factors would be unfeasible to do explains the reason why RSM optimization in culture media design is limited to 3-5 factors (Table 1).

#### 1.1.4 Artificial neural network

Artificial neural networks (ANN) are based on the structural aspect of the network of neurons in the brain. It's a mathematical system that adapts to the information flowing through the network, during the learning "stage". Given a set of training data the network learns to output certain data based on the input given, ANN are useful in culture media design because they are able to compute and learn every type of function, acting as a black box model for solving complex functions that describe microorganism metabolisms<sup>38</sup>.

The structure of the neural network its comprised in layers of "neurons", a "neuron" is a mathematical function that model the functioning of a biological neuron, that computes the so called activation value. The first layer of the structure it's called the input layer were its given the initial information, this layer of neurons is then connected to other layers until it reaches the output layer.

There are many types of neural networks Fig. 3 shows a simplistic structure for a multi layered perceptron neural network<sup>39</sup> which comprises multi layers of connected neurons.

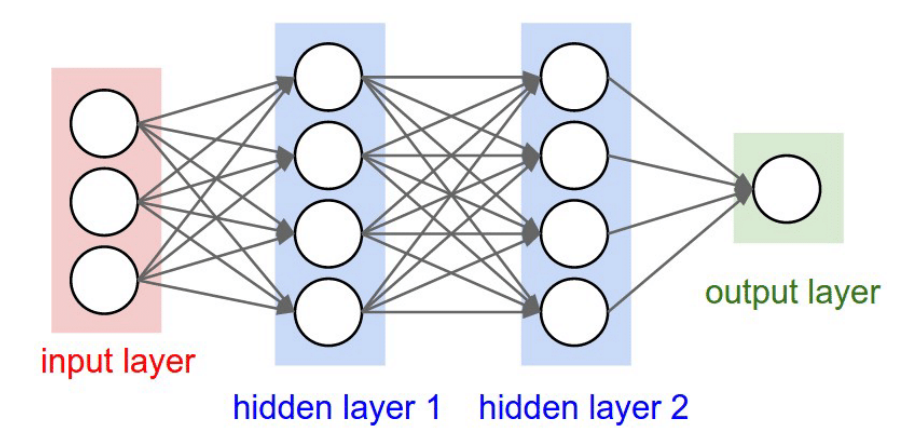


Figure 3 - Multi layered perceptron neural network

The activation value of a neuron is comprised by the sum of all connections values from the previous layer, a connection value is given by the activation value from the originating neuron and a weight value associated to that connection as presented by Eq. 9.

$$A = \sum_{i}^{n} wiai \tag{9}$$

Where A is the activation value of a neuron, n is the total number of neurons in the previous layer, w is the specific weight associated to a connection  $\{i\}$  and a the is the activation value from the neuron were connection  $\{i\}$  originated in the previous layer. The activation value is also subjected to an activation function that is mainly there to convert an input signal to an output one that can be used by the network, the activation function adds a layer of non-linearity, without this the neural network would be nothing more than a one-degree polynomial function, being just able to solve linear functions. The most used activation function is the sigmoid function (Eq. 10) that comprises the activation value between 0 and 1.

$$\sigma(A) = \frac{1}{1 + e^{-A}} \tag{10}$$

The neural network then learns to give a desired output value by running a set of learning data, utilizing a technique called backpropagation, the weights of each connection are modified so the network outputs the respective desired value. The objective is then, like RSM, to predict new data. An example of culture media design using ANN is the enhance of production of Avermectin B1b by *Streptomyces avermitilis*<sup>30</sup>. Also, various studies were conducted comparing RSM to ANN, showing that ANN as an overall better performance that RSM, with higher optimization and precision in predicted values<sup>40</sup> 41 42.

ANN is able to process large amounts of data, which is suited to conduct culture media design, although studies using ANN with more than 3-5 factors (Table 1) are, to our knowledge, inexistent in the literature. This is due to the fact that an ANN needs an initial set of training data, usually CCD is used to create this training set, needing a higher number of experiments the more factors we have in study, which can be costly and time consuming. The access to the training data is the main limitation factor in culture media design using ANN.

#### 1.1.5 Genetic Algorithm

Genetic algorithm (GA) mimics the process of natural selection and it's based in the principle "survival of the fittest" Different factors (genes) are encoded in a string (chromosome), the best performing individual is unchanged and the rest can "mate" in performance order.

The GA optimize for each generation the values of a fitness functions using mainly three types of rules to create the next generation:

- Selection rule, selects the individuals known as parents that contribute to the population of the next generation.
- Crossover rule combines two parents to form children for the next generation.
- *Mutation rule* applies random changes to individual parents to form children.

Fig. 4 represents the basic workflow of a genetic algorithm<sup>44</sup>.

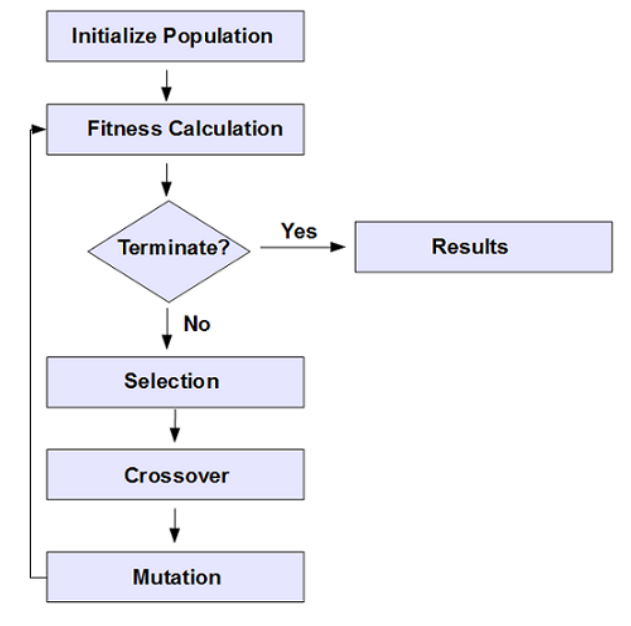


Figure 4 - GA basic flow scheme

Having the previous scheme (figure 4) as example, a generic algorithm can be implemented into culture media design (Figure 5).

Fig. 5 shows how a genetic algorithm can be implemented into culture media design<sup>26</sup>

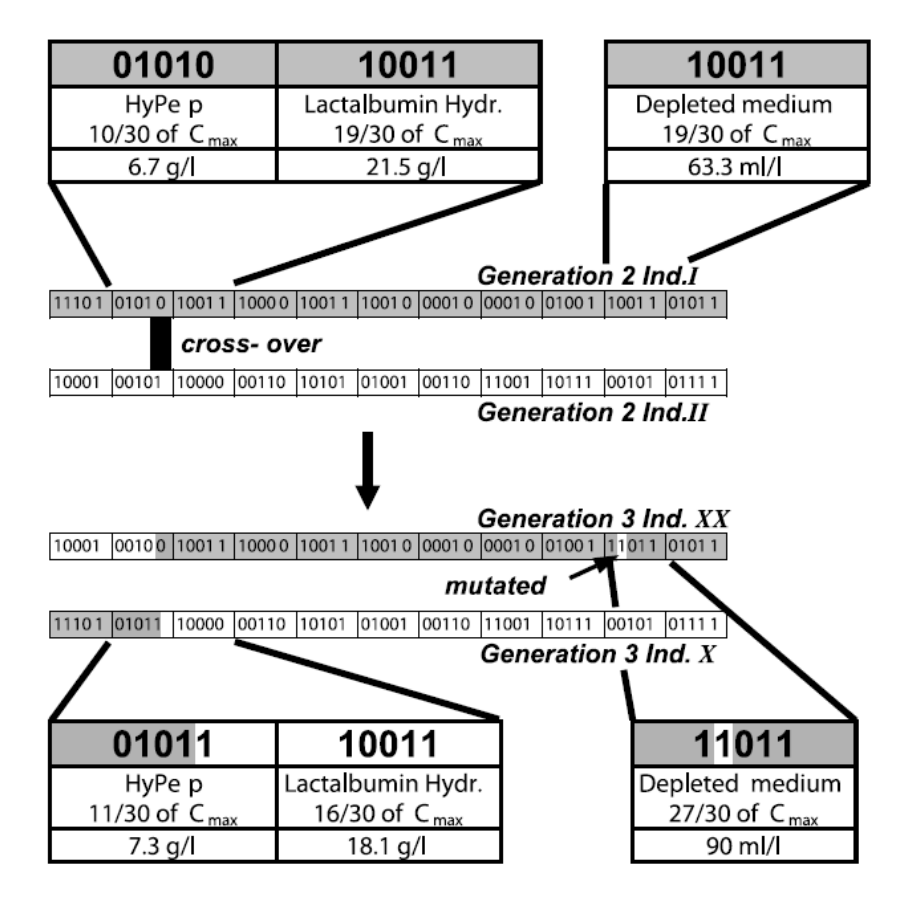


Figure 5 Example of culture media optimization using GA

In this example, the factors encoded were media components concentrations and the parents were selected for maximum cell density and growth rate (fitness function). For every generation a new set of media components was created and tested.

The main advantage of the GA is that, there is no guessing between each experiment as the direction of experiments is set automatically by experimental data, like so, the error between predicted and experimented values doesn't exist, unlike RSM that relies on a second order model to predict the response of complex cell metabolisms, with an increasing number of factors this can often result in poor estimation of optimal formulations<sup>45</sup>, this is not a limitation in the case of GA. Various studies were carried out for culture media design using GA<sup>26</sup> <sup>29</sup> <sup>28</sup> <sup>7</sup>, and although these studies shows good optimization values and higher number of factor when compared with other methods the main downside is the high number of experiments needed (Table 1).

Various studies were conducted comparing RSM coupled with GA (RSM-GA) and ANN coupled with GA (ANN-GA), were the genetic algorithm is used to optimize the mathematical models created by RSM and ANN. In these studies, ANN-GA performed better than RSM-GA<sup>32</sup> <sup>31</sup>(Table 1), making ANN-GA one of the best methods to use in culture media design.

#### 1.2 Metabolic modelling methods

All the culture media design methods described above are empirical in nature, i.e. they disregard knowledge on the biological mechanisms underlying cell growth and product synthesis. They rely instead on intensive experimentation to acquire cause-effect data for a very high number of media modifications. A step further could be the use of more rational design methods based on metabolic networks which are currently widespread in the literature <sup>46 47 48</sup>. The reconstruction of these networks allows to understand the interconnectivity and functional relationships between all biochemical reactions of a biological system. It is currently relatively easy to synthesize a detailed metabolic network of most of the cell lines/strains used for industrial production. In some organisms, a genome scale reconstructed metabolic network can be found in specific databases like BIgG (Genetic and Genomic knowledgebase of large scale metabolic reconstructions) <sup>49</sup>.

A metabolic network is a system where metabolites (nodes) are linked to each other by enzyme catalysed reactions (edges) where directionality of connection means mass conversion (arrow) (see Fig. 6 for illustration). Reactions that transform metabolites within the system are considered internal reactions, while reactions involving the transport of metabolites in and out of the system are considered exchange reactions. Figure 6 illustrates this concept with 5 internal metabolites (A, B, C, D, P) and 4 external metabolites (Aext, Bext, Dext, Pext)<sup>50</sup>.

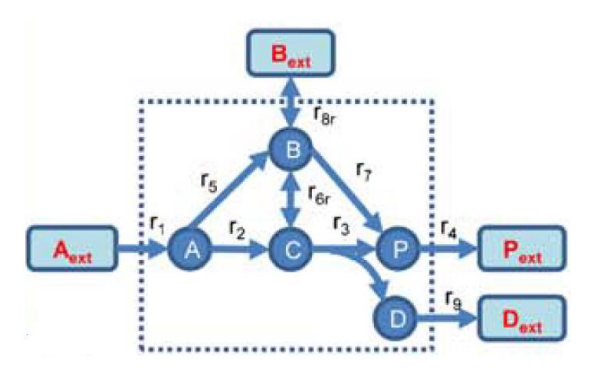


Figure 6 - Example of a simple metabolic Network

In this example reaction  $r_1$ ,  $r_4$ ,  $r_8$ , and  $r_9$  are considered exchange/transport reactions while the other are the internal reaction. The analysis of a metabolic networks is based on the principle of mass conservation of internal metabolites within a system<sup>9</sup>. Under the hypothesis of a well-mixed system, the general material balance equation applies (Eq. 11).

$$\frac{d}{dt}C = S \times r - \mu \times C \tag{11}$$

Where C is the metabolite concentration vector, r is the reaction rate vector,  $\mu$  is the specific growth rate and S is the stoichiometry matrix. The stoichiometry matrix S contains the stoichiometry of the network metabolites in each reaction, where the rows are the network metabolites and the columns are the network reactions.

Eq.12 illustrates the stoichiometry matrix for the metabolic network of Fig. 6.

At steady state, there is no accumulation of internal metabolites in the system and Eq. 11 can be simplified into Eq. 13.

$$S \times r = 0 \tag{13}$$

An additional restriction is needed (Eq. 14), due to thermodynamic constraints stating that irreversible reactions  $\{j\}$  have to proceed in the appropriate direction and require to have positive flux values

$$rj \ge 0 \tag{14}$$

There are 3 main techniques to solve Eq. 13 with de thermodynamic restriction (Eq. 14): metabolic flux analysis (MFA), flux balance analysis (FBA) and elementary mode analysis (EMA). These are briefly reviewed in the next sub-sections.

#### 1.2.1 Metabolic flux analysis (MFA)

In MFA the flux vector is divided into two vectors, a vector containing the measured metabolic fluxes  $r_{\rm m}$ , and a vector contain all the unmeasured fluxes  $r_{\rm u}$ , in this technique we solve Eq. 13 as:

$$S_u \times r_u = S_m \times r_m \tag{15}$$

With the  $S_u$  and  $S_m$  being the stoichiometric matrix of the unmeasurable and measurable fluxes respectively. We want to measure enough fluxes so that, the matrix  $S_u$  becomes invertible<sup>51</sup> and we can solve Eq. 15 like Eq.16:

$$r_u = -S_u^{-1} \times S_m \times r_m \tag{16}$$

Then we can obtain the unmeasurable flux vector  $r_u$  by solving Eq 14 15 and 16 in a system. MFA relies on measuring enough metabolic fluxes until we can calculate the unmeasured ones. Note that this technique only obtains a single metabolic flux vector for a specific growth condition, changing this growth condition will result in a different  $r_m$  vector leading to a different metabolic flux vector, an example of this is the study by Wilkens et al.<sup>52</sup>, lactate production was compared in a CHO cell line grown on two different substrates, namely glucose and lactose.

MFA has been applied in the context of culture media design as a "screening of factors" approach. MFA is typically applied for in-depth analysis of the effect of media factors on carbon flux distribution<sup>53</sup> <sup>54</sup>.It is however not a technique that can be applied for quantitative design of media composition.

#### 1.2.2 Flux balance analysis (FBA)

FBA is a technique that can be used for undetermined systems, i.e. when measured fluxes are not enough to invert matrix  $S_u$ . FBA implies an optimization according to some objective function alongside several flux constraints, such as, substrate consumption, product secretion, thermodynamic constraints, etc. Like MFA, FBA calculates one flux vector for a given growth condition. Fig. 7 illustrate a typical FBA problem for the small network shown of Fig.  $6^{50}$ :

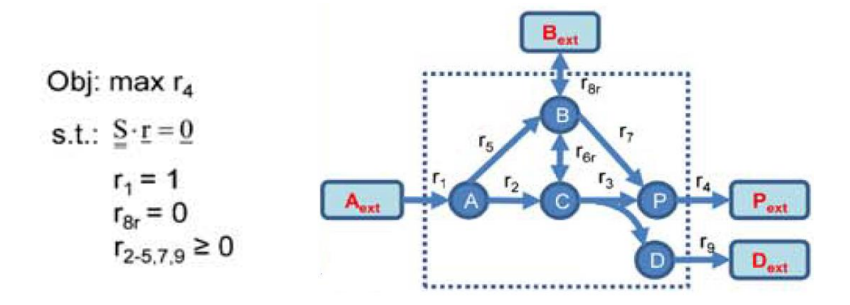


Figure 6 - FBA example, restrictions and objective function

In this example our objective function is to maximize the production of the metabolite  $P(r_4)$  while applying substrate consumption  $(r_1)$ , product excretion  $(r_{8r})$  and thermodynamic  $(r_{2-5,7,9})$  constrains.

The main challenge of this approach is to define an objective function that best describes the metabolism of a given growth condition<sup>55</sup> <sup>56</sup>.FBA was successfully implemented to develop a culture media supporting high cell density growth of Bacillus coagulans<sup>57</sup>.

#### 1.2.3 Elementary mode analysis

Elementary modes of a cell are defined as the unique set of reactions to support steady state operation of a metabolic network. Fig. 8  $^{50}$  shows all elementary modes present in the simple network of Fig. 6.

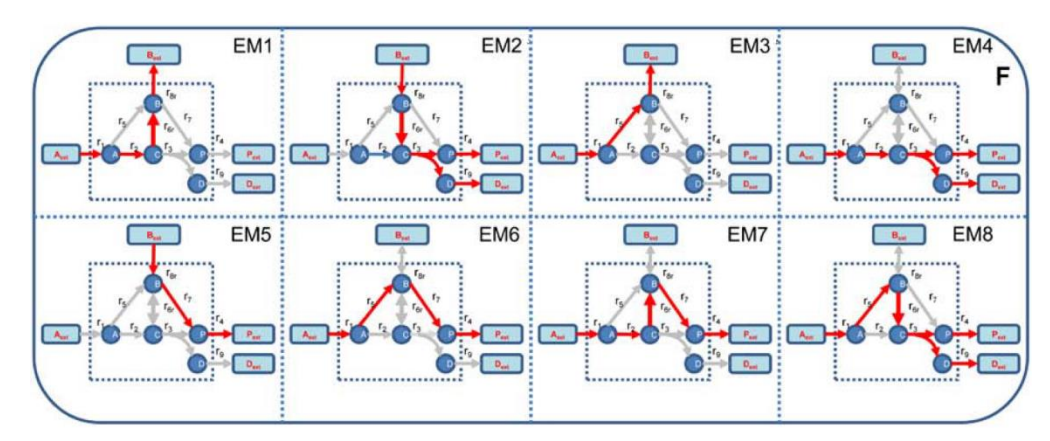


Figure 7 - Elementary modes of the Fig. 6 network

The universe of solutions of Eq. 13 together with the inequality constraint (Eq. 14) takes the form of a convex polyhedral cone<sup>58</sup>, containing an infinite number of solutions, i.e. the admissible flux space . Fig. 9 represents the admissible flux space for the network in Fig.6.

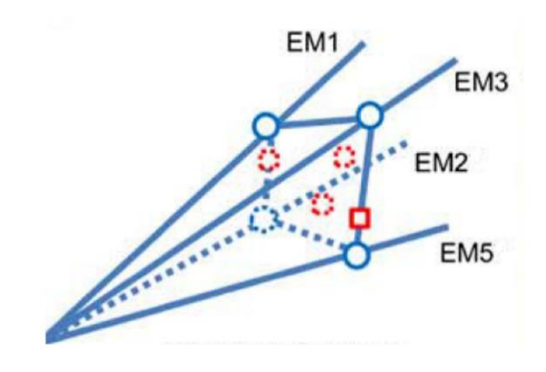


Figure 8.- Admissible Flux Space of the Fig. 6 network elementary modes

Elementary modes must also obey to the non-decomposability constraint. This non-decomposability constrain means that one EM vector cannot be described by other two or more vectors, meaning that each elementary mode its unique in the network.

After EMs calculation we obtain the EMs matrix that has all the EMs of the metabolic network Eq.17.

$$\underbrace{EM_1 \quad EM_2 \quad EM_3 \quad EM_4 \quad EM_5 \quad EM_6 \quad EM_7 \quad EM_8 }_{f_1}$$

The rows of the EM matrix represent metabolic reactions while the columns represent the elementary modes of the network. The values in the matrix represent the "weights" (i.e. participation strength) of a given reaction in a given EM. Note that the EM1 vector  $(1,1,0,0,0,-1,0,1,0)^T$  may be translated into a flux vector  $(2,2,0,0,-2,0,2,0)^T$  by multiplying a positive scalar factor, for example 2. Negative reaction "weights" apply only for reversible reactions, meaning that the particular reaction takes place in the opposite direction of the positive flux direction in that particular EM. Flux calculations are thus obtained by applying a linear combination of EMs according to Eq.18

$$r = \sum_{i} \lambda_{i} E M_{i} \tag{18}$$

With:

$$\lambda \ge 0 \tag{19}$$

There is a parallelism between Eqs. 18-19 and steady state Eqs 13-14. There is however a fundamental difference when doing flux calculations by applying EM analysis. EMs embody knowledge on regulation of metabolic processes. This is so because one EM is interpreted as a metabolic state, i.e. it is not only the metabolic fluxes but also the genes, mRNAs, proteins, that support that particular steady state flux distribution. For example, Tunahan Çakır et al.(2007)<sup>59</sup> correlated transcriptomic data to active EMs in *Saccharomyces cerevisiae*.

#### 1.4 M.Sc. thesis objectives

The general objective of this thesis is the development of a rational design method for culture media composition customized to the cell line and/or product. This method should act as a proof of concept for the future development of a toolbox. Instead of an empirical design approach where culture media composition is optimized resorting to intensive lab experimentation, the goal here is to develop an *In silico*, experiment-free culture media design method. Given that the knowledge of the metabolic network is easily available in public domain, this novel methodology should be based on prior knowledge of the metabolic network of the target cells. Moreover, since the elementary modes embody additional information on regulation, the elementary modes framework will be privileged over the MFA or FBA techniques. As such, the specific thesis objectives are the following:

**Objective 1**: Development of an *In silico* culture media design method based on prior knowledge of the metabolic network that drastically reduces the experimental activity for culture media optimization. In limit it should be experiment-free.

**Objective 2**: The *In silico* culture media design method should allow to compute culture media formulations customized to the cell line and/or product expressed by the cell line.

**Objective 3**. The method to be developed should be based on elementary modes framework. The advantage of the EM framework is the inclusion of high level regulatory information that is easily accessible.

**Objective 4**: Implement the EM culture media design method in MATLAB. The input information is the metabolic network of the target cell line including detailed information of its biochemical composition and the synthesis of the target product. The output of the method is theoretical culture media formulations for the particular cell line and product.

**Objective 5:** Apply the method/tool to design *In silico* culture media formulas for Chinese Hamster Ovary (CHO) cells as illustrative case study and compare computed culture media formulations with literature data.

## 2. SBEMedia: a toolbox for *In silico*

## culture media design

In this thesis the method for the SBEMedia toolbox was developed for *In silico* experiment-free culture media design. The methodology applied in this thesis is based on the concept of elementary modes and the respective footprint. Fig. 10 illustrates a cell growth elementary flux mode for Chinese Hamster Ovary Cells (CHO). The nodes in green represent the exchange of materials with the extracellular media for the cell to be able to grow according to the particular elementary mode.

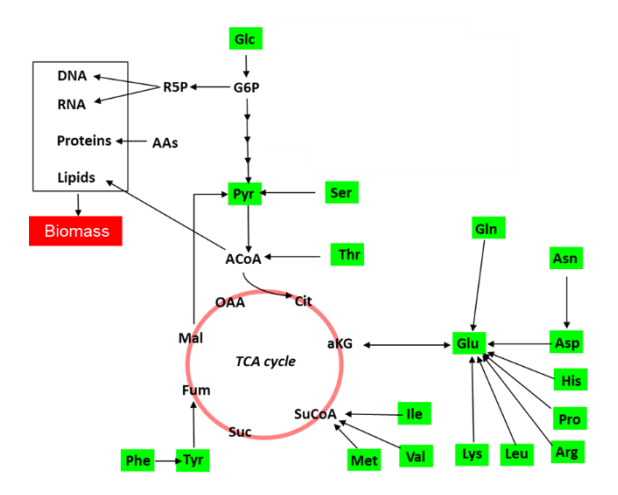


Figure 9 - Example of a Chinese Hamster Ovary Cell elementary mode

The SBEMedia toolbox implements the following sequence of steps to compute *In silico* culture media formulations based on prior knowledge of the metabolic network:

- **Step 1. Input metabolic network**: The metabolic network comprising a list of representative metabolic reactions including i) the synthesis of the target product and ii) the exchange reactions of media components for the synthesis of the target product, are inputted to the system;
- **Step 2. Computation of elementary modes:** The full set of elementary modes of inputted metabolic network are calculated using elementary mode analysis algorithms; the resulting full set of elementary modes displays the full range of possible metabolic states for the cells to realize their biological function.
- **Step 3. Computation of the** *footprintome***:** The metabolic footprint of each elementary mode is computed and merged together in a full matrix comprising all possible modes to interact with the extracellular environment. The full set of footprints is denominated "*footprintome*".

- **Step 4. Automatic** *footprintome* **reduction:** The *footprintome* is reduced based on three steps: eliminating EMs that don't produce the target product (this will later be explain), eliminating EMs that are thermodynamically unfeasible and clustering EMs that have the same phenotype (same list of external metabolites being produced and consumed).
- **Step 5. Case-dependent** *footprintome* **reduction based on optimal metabolic criteria.** In this step, a subset of elementary modes and respective footprints are selected such as to enforce a desired metabolic state. This step is case dependent and implies the definition of optimal metabolic criteria for the target cell
- **Step 6.** *In silico* **culture media formulations:** Computation *In silico* of culture media composition based on the final reduced *footprintome*.

All methods were implemented in MATLAB version  $R2019a^{60}$ . What follows are the details of each step provided.

#### 2.1. Input metabolic network

The metabolic network is inputted as a MATLAB data structure with a list of reactions. To illustrate this, we specify below the metabolic reactions of the simple network of Fig. 6

```
Network = {

Internal reaction:

'A -->B'

'A -->C'

'B -->P'

'C -->P+D'

'C<-->B'

External/Transport reactions

'-->A'

'<-->B'

'P-->'

'D--->'
```

The exchange reactions, which must be placed in the end of the reactions list, implies a decision on the identity of the culture media components whose concentrations need to be optimised.

A more realistic metabolic network, considering the production of biomass and product is described below in the CHO case study.

#### 2.2 Computation of Elementary modes

The metabolic network is parsed and processed into a MATLAB data structure using the *efmtool* package version 4.7.1. This MATLAB package is freely available for academia and may be accessed at <a href="https://csb.ethz.ch/tools/software/efmtool.html">https://csb.ethz.ch/tools/software/efmtool.html</a>. The *efmtool* package builds: i) a list of metabolic reactions, separated as intracellular and extracellular and extracellular, iii) creates the stoichiometric matrix **S** (Eq. 12) and internal and external stoichiometric submatrices. It also computes the elementary modes and delivers the result in the form of elementary modes matrix EM (Eq. 17). The method used to calculate the EMs is described in detail in Terzer et al. <sup>61</sup>. The determination of elementary modes by this method suffers from the computational explosion problem <sup>62</sup>. It can be thus applied only to small and medium scale networks, it cannot be applied to genome scale networks.

#### 2.3 Computation of the *footprintome*

Once the network elementary modes are computed, the next step is the computation of the *footprintome*. The footprint of an elementary mode may be seen as the extracellular phase modification pattern characteristic of the particular elementary mode. This footprint is computed from the subset of exchange reactions, in and out, and their respective weights in the EM matrix. Thus the first procedure is to reorganize the EM matrix by considering the exchange reactions only, and eliminating all others, resulting in Eq. 20.

$$EM^{exch} = \begin{bmatrix} \frac{1}{10} & \frac{1}{1$$

The stoichiometric matrix S is also reorganized by considering only the stoichiometry of the exchange reaction (Eq.21).

$$S^{exch} = \begin{bmatrix} S_{\frac{1}{2}} & S$$

The footprintome of the cell results from the multiplication of these two matrices (Eq.22):

$$footprintome = -S^{exch} \times EM^{exch}$$
 (22)

This operation eliminates all the intracellular metabolites, resulting in macroscopic reactions defining the stoichiometric conversion of extracellular substrates into extracellular products. Note that the minus sign is required because the metabolic reactions are defined in the perspective of the interior of the cell, i.e. the positive direction of an exchange flux is from the extracellular to the intracellular phase. With the minus signal the perspective is flipped, such that all culture media substrates take a negative stoichiometric coefficient, whereas all products of the network take a positive coefficient. The final result is thus a matrix with rows representing culture media components, columns representing elementary mode, and the matrix values are stoichiometric conversion factors.

#### 2.4 Automatic footprintome reduction

The *footprintome* is typically a large matrix that comprises all possible interaction modes with the culture media. It may be reduced automatically by applying the following criteria:

- *Elimination based on selected product*. Footprints that do not produce the target product are not useful for design purpose thus eliminated. The target products are typically biomass and/or recombinant product. As example, if the objective is to design a cell growth culture media, then only elementary modes with biomass production are selected for further analysis while all other eliminated. After this reduction step, the *footprintome* is normalized column wise by dividing the footprint vector by the stoichiometric coefficient of the target product. In this way the footprint of each EM is interpreted as the quantities of substrates consumed and sub-products produced per unit of target product synthesized.
- **Thermodynamic reduction**. In this step a thermodynamic elimination of elementary modes based on the Gibbs free energy of reaction of the metabolites in each EM is performed. All elementary modes with positive Gibbs free energy of reaction are considered unfeasible thus eliminated. More details on the calculation of  $\Delta G^{o}_{r}$  are provided next.
- Clustering based on footprint similarity (Pattern Clustering). Many elementary modes footprints have the same phenotype (same list of external metabolites being produced and consumed). These are clustered together.

# 2.4.1 Calculation of elementary mode Gibbs free energy of reaction ( $\Delta G^{0}r$ )

The change in the Gibbs free energy of formation of a substance is the difference between the free energy of a substance and the free energies of its elements in their most thermodynamically stable states at standard-state conditions. The Gibbs free energy of reaction,  $\Delta G^0_r$ , is a measure of reaction spontaneity ( $\Delta G^0_r < 0$ ) for constant pressure and temperature processes which describes the majority of the biological systems<sup>63</sup>.

$$aA + bB \rightarrow cC + dD$$

For reaction 1, the standard Gibbs free energy of reaction is given by Eq. 23:

$$\Delta G^{0}r = c * \Delta G^{0}f(C) + d * \Delta G^{0}f(D) - (a * \Delta G^{0}f(A) + b * \Delta G^{0}f(B))(23)$$

Where  $\Delta G^0_f$  is the metabolite standard Gibbs free energy of formation.  $\Delta G$  depends only on the difference in free energy of products and reactants (or final state and initial state).  $\Delta G$  is independent of the path of the transformation<sup>64</sup>. With this in mind, the EMs are considered to be macroscopic reactions that transform a number of extracellular substrates into a number of extracellular products. The  $\Delta G^0_r$  was calculated for each EMs and whenever  $\Delta G^0_r > 0$  (nonspontaneous reactions) the respective EM is eliminated from the list. The metabolite standard energy of formation data were taken from the *eQuilibrator*<sup>65</sup> database, that uses the group contribution metodologies<sup>66</sup> to estimate the Gibbs free energy of formation of metabolites.

For IgG the  $\Delta G^0_f$  value was not found in the literature alongside with that of biomass of CHO cells. For these complex products the  $\Delta G^0_f$  was computed from the respective reaction of formation in the network of IgG (reaction 78) and biomass (reaction 69) respectively, as shown in Eq. 24.

$$\Delta G^0 f = \sum_{i}^{n} ai \times \Delta G^0 f(Mi) \tag{24}$$

With n being the number of metabolite reactants in the reaction, ai are stoichiometric coefficients and  $\Delta G^0_f(M_i)$  the standard Gibbs free energy of formation of the metabolite i.

#### 2.4.2 Clustering based on phenotype similarity.

In this step, after grouping the footprints together based on their phenotype the centroid position of each cluster is computed based on the arithmetic average of the metabolite values (Eq. 25).

$$F = \frac{\sum_{i}^{n} footprint_{i}}{n}$$
 (25)

With F being the centroid footprint and n the number of footprints under consideration. Note that Eq.21 will also be applied to do the arithmetic average of all EM in a *footprintome* in chapter 3.4, "Comparison with experimental data", alongside a second method, the weighted average of the *footprintome* by the  $\Delta G^0$ r of each EM, shown in Eq. 26.

$$F = \frac{\sum_{i}^{n} \Delta G^{0} r_{i} \times EM_{i}}{\sum_{i}^{n} \Delta G^{0} r_{i}}$$
 (26)

# 2.5 Case-dependent *footprintome* reduction based on optimal metabolic criteria

A much smaller set of elementary modes and respective footprints are selected based on optimal metabolic criteria. The optimal metabolic criteria are case dependent. A typical objective might be the elimination of undesired metabolic byproducts secreted to the culture media. This is achieved by eliminating all elementary modes that produce the particular byproduct. In the CHO case study, hypothetical culture media that eliminate the production of lactate and ammonium is targeted. Another important criteria, especially for animal cell lines, is the media osmolarity. Culture media formulations that lead to a large increase in osmolarity should be eliminated (more to this will be discussed in the case study).

#### 2.6 *In silico* culture media formulations

The final step is the computation of culture media formulas from the remaining EMs. At this stage only a small set of elementary modes survives the elimination/selection process.

It is possible to choose an optimum EM from the remaining set of EMs. For each criteria implemented, elementary modes were given a score value between 0 and 1, dependent on the criteria value of the respective elementary mode. The lower the score value, the better the criteria value of an elementary mode is, compared with other EMs. If the objective is to minimize the criteria value, then Eq. 27 is applied:

$$Score_i = \frac{Criteria_i}{\max(Criteria)} \tag{27}$$

With Score and Criteria, being vectors containing the score and the criteria values of the EMs for the criteria{i} and max(Criteria) being the highest values in the Criteria vector.

In cases where we want to maximize a criteria value, Eq.28 is applied:

$$Score_i = 1 - \left(\frac{Criteria_i}{\max(Criteria)}\right)$$
 (28)

The Total Score vector, comprises the final score for each EM, it is the sum of the score vectors of all criteria implemented (Eq. 29).

$$Total Score = \sum_{i}^{n} Score_{i}$$
 (29)

With n being the total number of criteria implemented.

The EM with the lowest total score value is chosen as the optimum one. Note that the final culture media formula is a vector whose elements represent the stoichiometric quantities of culture media components per unit of target product produced. To transform it in concentrations we need to multiply the culture media vector by the concentration of the target product,  $(C_{product})$ , as shown in Eq. 30.

$$C = Op \times c_{product} \tag{30}$$

With C being the concentration vector of metabolites and Op the optimal EM chosen.

## 3. Results and discussion

# 3.1 Chinese Hamster Ovary Cells (CHO) metabolic network

To illustrate the application of this method, a Chinese Hamster Ovary (CHO) cell line expressing an antibody (IgG) was selected as a case study. CHO cells are currently the workhorse in the biopharmaceutical industry to produce monoclonal antibodies. It is probably the most important cell line in the biopharmaceutical industry today<sup>67</sup>.

The metabolic network used in this thesis was adapted from the work published by Duarte et al.<sup>68</sup>. In this study the authors adapted and validated the CHO metabolic network from previous published works (Quek et al.<sup>69</sup>, Sengupta et al.<sup>70</sup>, Zamorano et al.<sup>71</sup>) and complemented the model using <sup>1</sup>H-NMR (Proton nuclear magnetic resonance) exometabolomic analysis to quantify supernatant metabolites along culture time, under butyrate-treated conditions.

In this thesis the network was simplified by eliminating ATP, NADH, NADPH and FADH2 and respective oxidative phosphorylation reactions. Thus the simplified metabolic network closes the carbon and nitrogen balances, but does not close the oxygen and hydrogen balances. The simplified CHO metabolic network has 114 reactions (79 intracellular and 35 exchange reactions) and 81 metabolites (46 intracellular and 35 extracellular). The full list of reactions is provided in Appendix A.1. The target network "products" are biomass (X) and antibody (IgG). The synthesis reaction of CHO biomass sets the amounts of compounds in nmol required to synthesize 1 unit of CHO biomass. One unit of CHO biomass corresponds to  $10^6$  cells or a CDW of 271  $\mu$ g.

#### Reaction 2 - Biomass synthesis reaction

 $160.1015 \ Ala + 235.2056 \ Glu + 70.3787 \ Gln + 174.6799 \ Gly + 114.9787 \ Ser + 147.4132 \ Lys + 157.4070 \ Leu + 82.6648 \ Ile + 91.8543 \ Arg + 169.492 \ Asp + 95.7754 \ Thr + 118.3569 \ Val + 40.0354 \ Met + 67.4027 \ Phe + 47.4956 \ Tyr + 36.2551 \ His + 55.559 \ Pro + 70.3787 \ Asn + 8.943 \ AMPRN + 4.878 \ Cholesterol + 14.9321 \ CMPRN + 4.0108 \ dAMP + 2.6829 \ dCMP + 2.6829 \ dGMP + 4.0108 \ dTMP + 0.813 \ DPG + 75.609 \ Glycogen + 16.9104 \ GMPRN + 18.699 \ PC + 7.046 \ PE + 0.271 \ PG + 2.71 \ PI + 0.813 \ PS + 2.168 \ SM + 8.943 \ UMPRN + 9.2297 \ Trp --> 1 \ X$ 

The IgG synthesis reaction reflects the amount of compounds in nmol needed to synthesize 1 mg of IgG.

#### Reaction 3 – Antibody IgG synthesis reaction

 $428.7 \ Ala + 362.75 \ Glu + 351.76 \ Gln + 516.64 \ Gly + 934.36 \ Ser + 472.67 \ Lys + 516.64 \ Leu + 175.88 \ Ile + 307.79 \ Arg + 296.8 \ Asp + 626.57 \ Thr + 714.51 \ Val + 65.954 \ Met + 285.8 \ Phe + 285.8 \ Tyr + 164.89 \ His + 505.65 \ Pro + 263.82 \ Asn + 142.9 \ Trp + 10.992 \ GDPFuc + 54.962 \ UDPNAG + 32.977 \ GDPMann + 21.985 \ UDPGal + 21.985 \ CMPSialic --> 1 \ P$ 

The culture media components that will be subject to optimization in the following section are those present in the exchange reactions with positive influx to the intracellular phase. These are:

Glucose (Glc), Glutamate(Glu), Serine(Ser), Lysine(Lys), Leucine(Leu), Isoleucine(Ile), Arginine(Arg), Aspartate(Asp), Threonine(Thr), Valine(Val), Methionine(Met), Phenylalanine(Phe), Tyrosine(Tyr), Histidine(His), Proline(Pro), Choline, Asparagine(Asn), Tryptophan(Trp) and Pyruvate(Pyr).

In the following sections, custom culture media will be developed for the specific cell line growth specified by reaction (2) and for the specific IgG specified by reaction (3) by determining the optimal quantities of the exchange compounds listed above. Obviously, these exchange compounds do not cover the complete set of media components in a typical CHO culture media, which has typically more than 100 components. In future studies, this network could be enlarged to include additional media exchange components.

#### 3.2 Computation of CHO Elementary Modes

The complete set of elementary modes was computed for the CHO metabolic network using the  $efmtool^{72}$ . The elementary modes count of medium and large metabolic networks can be very high, in the order of millions<sup>73</sup>. To facilitate the computation of elementary modes, it was considered two different scenarios:

- i) The metabolic network includes the biomass synthesis reaction only (without the IgG synthesis) resulting in the biomass elementary modes (biomass-EMs).
- ii) The metabolic network includes the IgG synthesis reaction only (without the biomass synthesis reaction) resulting in the product elementary modes (product-EMs).

By removing the biomass synthesis and IgG synthesis reactions of the network, further reactions needed to be removed in order to not create metabolic dead ends for specific intracellular metabolites. As a result, for the biomass producing network the IgG glycosylation reactions were also removed, resulting in a 106 reaction network (Appendix A, Table A.2), for the IgG producing network the lipid synthesis reactions were removed, as well as some reactions in the nucleotide synthesis and glycogen synthesis metabolisms, this also led to the removal of the Choline and Glyc3PC exchange reactions. The final number of reactions in the IgG producing network was 92 (Appendix A, Table A.3)

The final count of Elementary Modes obtained is shown in Table 4

Table 4 Elementary mode count of the biomass and product producing networks.

	Without	With
	ATP/NADH/NADPH/FADH2	<i>ATP/NADH/NADPH/FADH2</i>
Biomass-EMs	218 538	1 987 460
Product-EMs	313 523	1 768 927

To note that the inclusion of oxidative phosphorylation reactions increases very expressively the EMs count. The overall computation time for the biomass producing network increases from 30,420s to 267,63s, and in the IgG producing network from 27,72s to 206,80s, roughly a 10-fold increase in both networks. Although the computation time of EM for the more complex metabolic network wouldn't take a deterrent amount of time for the making of this work the computation of the respective *footprintome* visualizations would. For this reason, we have adopted in the proceeding studies the simplified version of the metabolic network.

Note also, that the number of final EMs is not dependent on the stoichiometry of the biomass or IgG synthesis reactions.

As an illustrative example, Appendix B, Table B.1, represents one EM from the biomass producing network that uses the minimum number of metabolic reactions required to synthesize 1 unit of biomass. This EM is potentially very efficient for cell growth using the minimum regulatory resources to synthesize one unit of biomass. Even so, only 42 from the 106 reactions in the network do not participate in this EM. By multiplying the elementary modes coefficients by the exchange reactions stoichiometry (reactions 73 to 106), one gets the EM footprint shown in Table 5. The metabolites in green are end-products secreted to the culture media, whereas the red metabolites are substrates needed to synthesize biomass. The footprint may be interpreted as the resources needed to synthesize one unit of biomass and respective by-products if the cells grows according to the EM shown in Appendix B.

Table 5-Footprint of the EM represented in Appendix B

Metabolite	Footprint (nmol/10 <sup>6</sup> cell)
X	1,00
Glc	-269,67
His	-37,17
Isobut	0,00
Ile	-84,75
Isoval	0,00
Leu	-161,33
Lys	-151,08
Met	-41,00
Phe	-254,08
Thr	-323,83
Trp	-9,50
Val	-121,33
CO2	972,83
NH4	0,00
Acetate	0,00
Ala	0,00
Arg	-311,33
Asn	-72,17
Asp	-342,50
Gln	0,00
Cit	0,00
Choline	21,42
Formate	0,00
Glu	-232,33
Glyc	0,83
Gly	0,00
Lac	0,00
Pro	-56,92
Pyr	0,00
Ser	-128,17
Tyr	0,00
Mal	0,00
Glyc3PC	0,00

# 3.3 Computation and reduction of CHO footprintome

The *footprintome* may be defined as, the complete set of footprints a cell may resort to, realize its physiological objectives. The *footprintome* is computed by repeating the process described in the previous chapter for the complete set of EMs. The footprint of each EM (a column vector) are stacked together in a large matrix in the final form of the *footprintome* matrix. Each footprint is a potential culture media "candidate", thus it is imperative to reduce as much as possible the size of the *footprintome* by eliminating nonessential footprints. The full set of EMs undergoes three steps of automatic reduction as described below for the biomass-EMs (A similar reduction procedure was applied to the IgG-EMs with final results presented in Appendix F Fig. F.1-F.2) as follows:

- The biomass-EMs (count = 218538) contain several EMs without biomass production. These were eliminated reducing the total EMs count to 211580. All columns of the *footprintome* are afterwards normalized by dividing by the biomass coefficient respectively. As a result, the biomass rows are always one, whereas the other rows read as nutrient consumption/production per unit of biomass production.
- The next step is the thermodynamic reduction. The  $\Delta G^0$ r was computed for each EM and those with nonnegative  $\Delta G^0$ r were eliminated. This step further reduced the EMs count to 203137. The result of this reduction is shown in Fig. 11. The  $\Delta G^0$ f values of each metabolite can be found in Appendix C.
- The next step is *footprintome* reduction by clustering based on phenotype similarity. Footprints that have the exact same list of substrates and end-products are clustered together. These clusters are averaged into a representative footprint by the arithmetic average (Eq. 25). This procedure ensures that the reduced set of footprints centroids (for simplicity sake during this work we will still be calling the footprints centroids as only footprints, although they are no longer representative of a singular EM) are linearly independent and characteristic of a unique cellular phenotype. This reduces the footprints count to 3488. This step was the one that achieved a higher degree of reduction. The result of this reduction is shown in Fig. 12

These results are summarized in Table 6.

Table 6. Automatic *footprintome* reduction results

	BIOMASS-EMS	IGG-EMS
BEFORE REDUCTION	218538	313523
ELIMINATION BASED ON SELECTED PRODUCT	211580	307404
THERMODYNAMIC REDUCTION	203137	307402
CLUSTERING	3488	4704

After the automatic reduction steps, 3488 potential cell growth footprints remain, which still is very high to test in the lab. Nevertheless, in a scenario of abundant resources it would be feasible to test them in a high throughput cell culture equipment such as the Sartorius AMBR® system.

Other studies in the literature have attempted EM reduction using different criteria. Hyun-Seob Song et. al. <sup>74</sup> proposed a reduction method based on yield analysis, in which the authors also compute EMs ratios of specific metabolites and use it to characterize different EMs phenotypes. The "yield analysis" method reduces EMs count to a small set representative of 99% of all phenotypic states. This reduction is however based on experimental data. Folch-Fortuny et al <sup>75</sup> proposed a method for discrimination of active EMs based on fluxomic datasets and tested it in *Escherichia coli* and *Pichia pastoris* cultures. It reduces the full set of EMs into a small number of representative EMs based on independent measurements of metabolic fluxes. This method explores the analogy of EM and principal component analysis of a measured fluxomics dataset. Ferreira et al. (2011)<sup>76</sup> proposed a method to discriminate active EMs also based on experimental measurements of metabolic fluxes. A reduced set of EMs is discriminated by maximizing the correlation of the EM weighting factor and measured media composition.

All the above methods are good options for EMs reduction when sufficient measured data of metabolic fluxes and/or metabolic footprints are available. Therefore, they could not be applied in this thesis as the objective in this thesis is to design *In silico* (100% experiment-free) the composition of culture media.

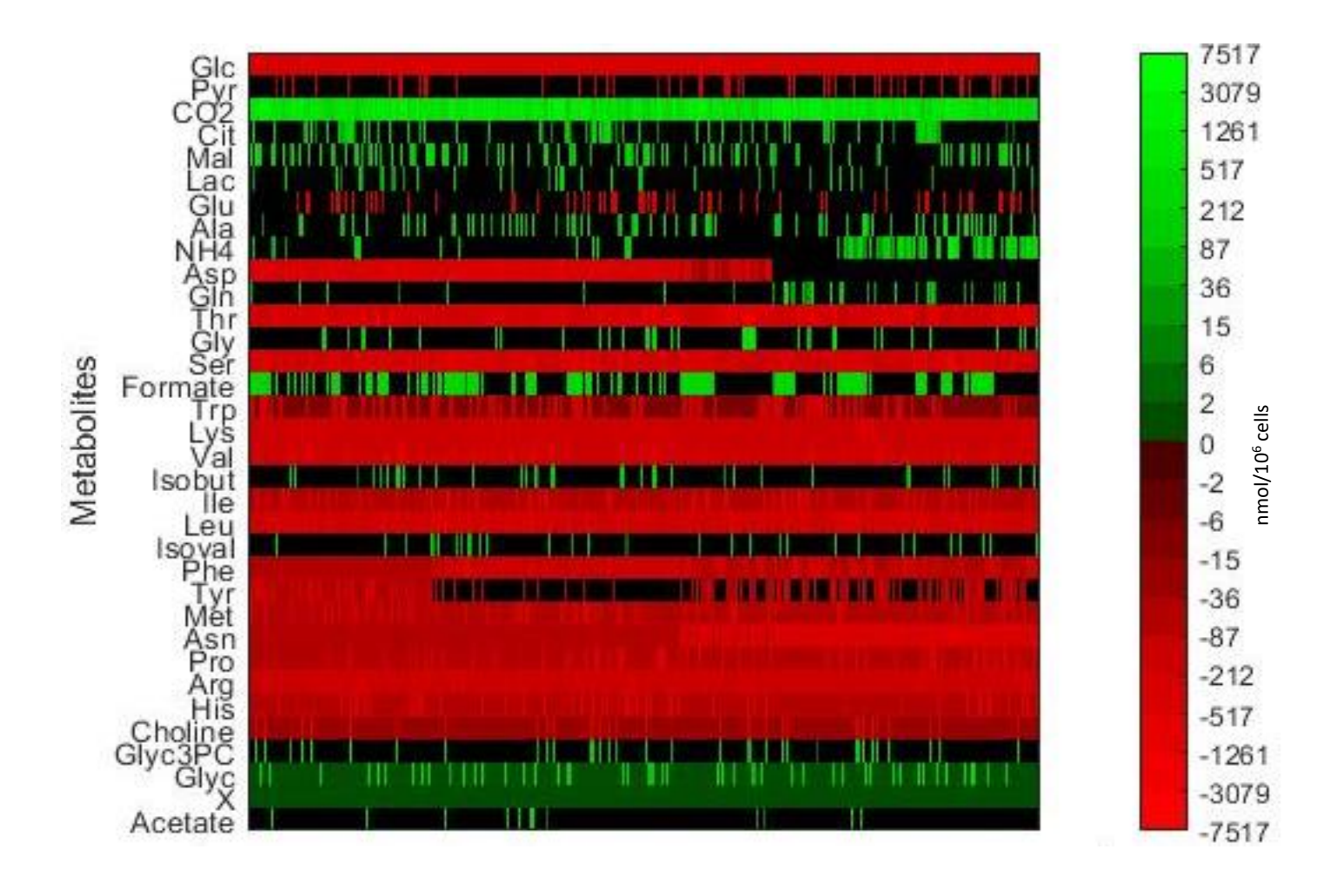


Figure 10 - Reduced footprintome for biomass production (normalized to unit) after 2 steps of reduction: Step 1- biomass production, Step 2-thermodynamic reduction. The columns represent the reduced set of EMs (203137). The colour green means that the compound is being produced by the EM. The colour red means it's being consumed by the EM. The black means it is neither consumed nor produced by the EM.

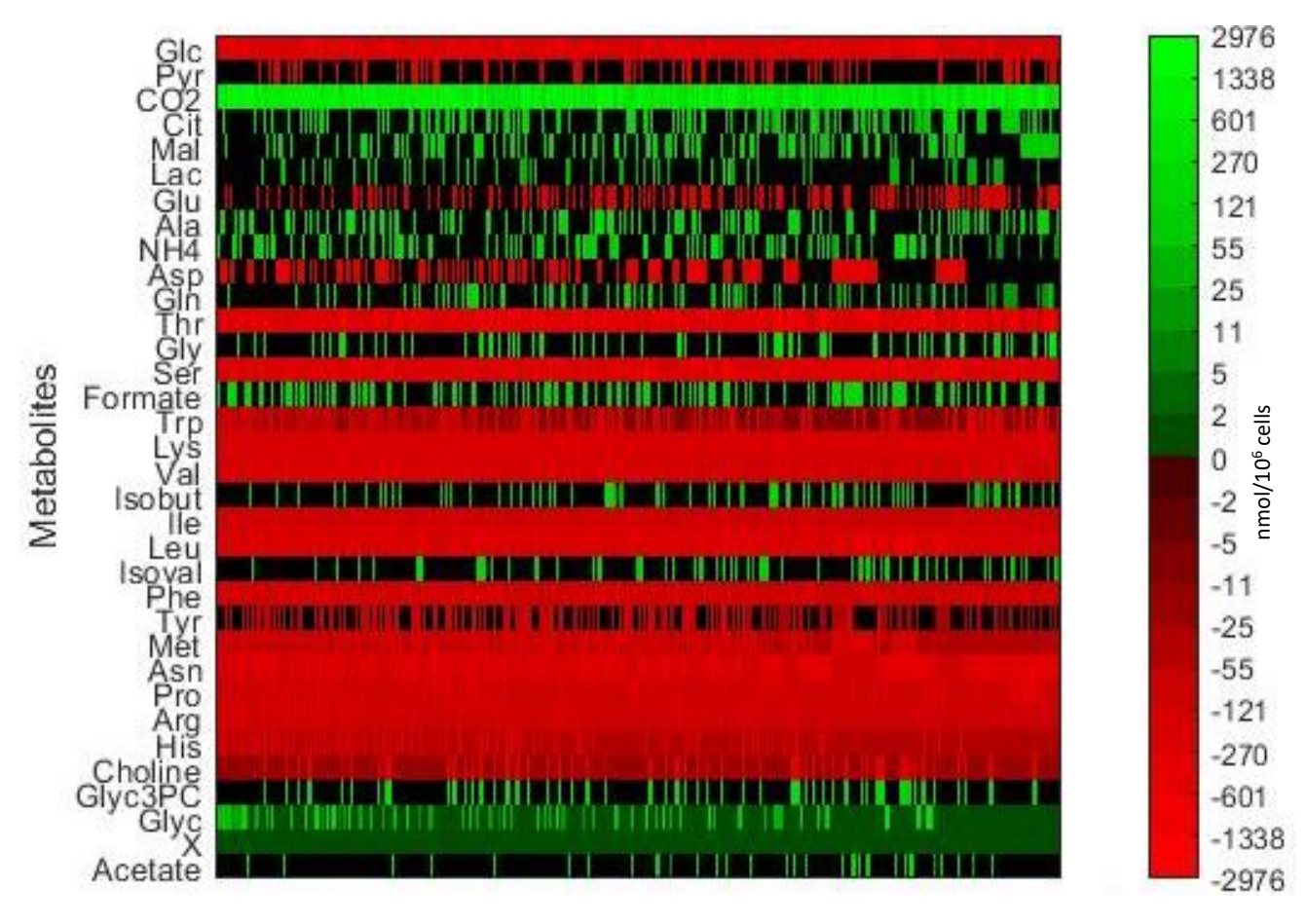


Figure 11 - Reduced footprintome for biomass production (normalized to unit) after 3 steps of reduction: Step 1- biomass production, Step 2-Thermodynamic reduction, Step 3-Pattern clustering with arithmetic averaging. The rows represent extracellular media components. The columns represent average EM clusters (3488). The green gradient represents compound production associated with the production of 1 biomass unit. The red gradient represents compound consumption to generate 1 biomass unit. The black colour means that the compound is neither consumed nor produced by the EM cluster.

# 3.4. Comparison with experimental data

The objective here is to compare the theoretical *footprintome* (computed from the metabolic network) with measured data of uptake/production rates of media compounds in CHO cultures (measured footprint). More specifically, the data published by Duarte et. al. <sup>77</sup>, who studied the metabolic response of CHO cells metabolism in experiments with varying concentration of asparagine and serine in the culture media, this data was adopted to validate the theoretical biomass growth *footprintome* after thermodynamic selection (Fig. 11). In order to compare the theoretical *footprintome* to a measured time point, it is required to average the full set of footprints into a representative footprint. Two different averaging methods were applied:

- i) Arithmetic average of all EM footprints (Eq. 25) in the *footprintome* of Fig. 11. The idea behind this method is that the number distribution of nutrient requirements in the *footprintome* is a measure of probability, thus the culture media formulation of a particular metabolic model corresponds to the mean concentration based on number.
- ii) Weighted average by the  $\Delta G^0$ r of each EM footprint (Eq. 26) in the *footprintome* of Fig. 11. The idea behind this method is that thermodynamically more favourable EMs have a higher contribution to the observed footprint.

Fig. 13A shows the overall results for the arithmetic average and the weighted average, compared with the measured foortprint data (Fig. 13B), that was obtained from the raw data published by Duarte et. al. (2014) (Appendix D), normalized by the cell growth rate.

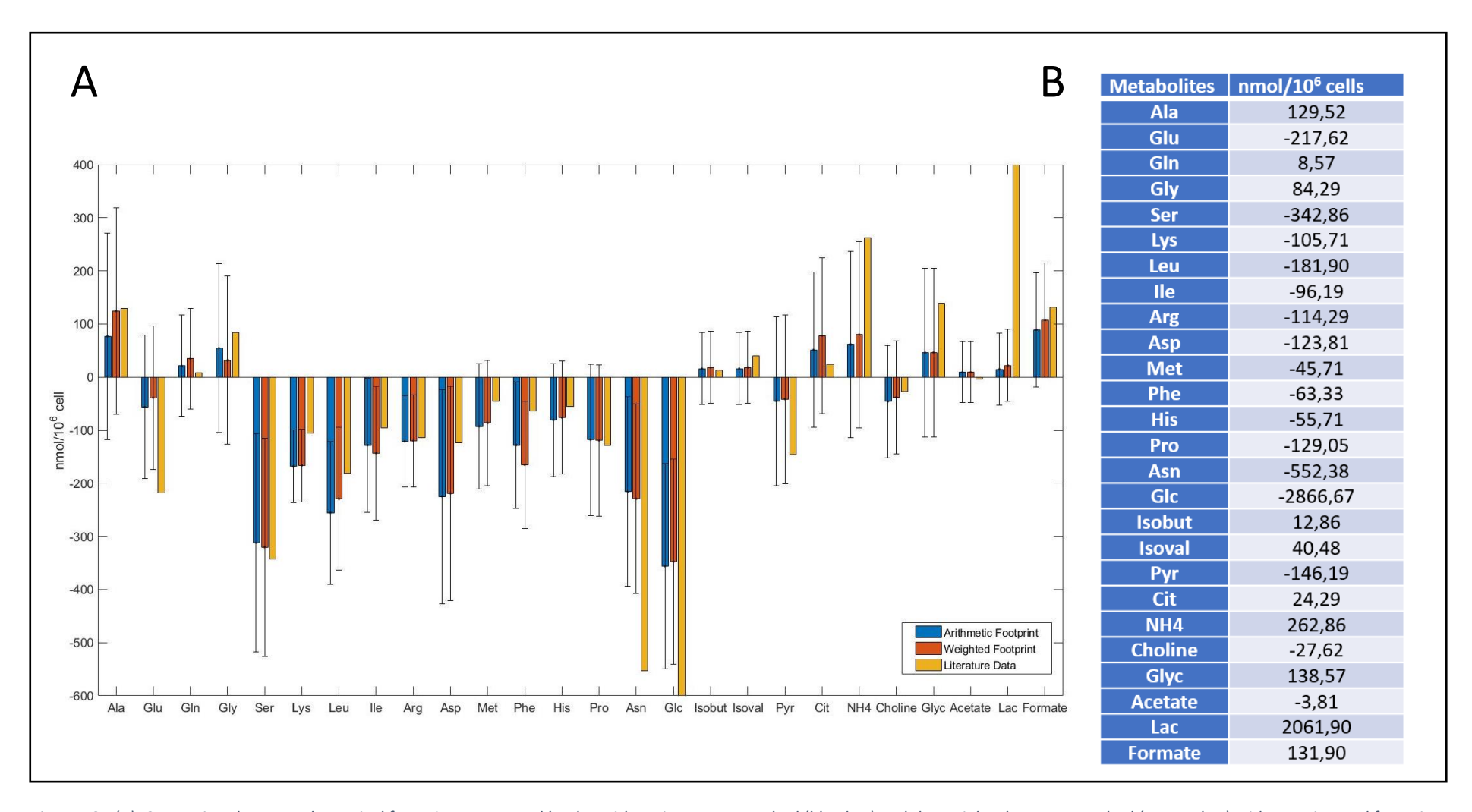


Figure 12 - (A) Comparison between theoretical footprints computed by the arithmetic average method (blue bar) and the weighted average method (orange bar) with experimental footprint (yellow bar). (B) Experimental footprint taken from Duarte et. al. (2014)<sup>58</sup>. The error bars correspond to the standard deviation of footprints in relation to the average

All in all these results show a remarkable concordance between the theoretical footprint and the measured footprint. Moreover, the measured footprint is within the variance interval of the theoretical footprints computed for most nutrients (exceptions discussed below) as shown by the error bars in Figs. 16A. It should be highlighted that the theoretical footprint was computed resorting to the metabolic network information only. It is completely *In silico* and experiment free.

The broad error bars displayed in Figs. (13A) reflect the variablity in theoretical footprints. Even if it is not possible to know *a priori* without any experimental evidence which are the "active EMs" used by the cells to grow, it is possible to determine the average theoretical footprint and theoretical variability around the mean.

The only large theory-measurement mismatch observed in Fig. 13A relates to the glucose and lactate nutrients. The measured footprint is characterized by a very high glucose consumption yield (-2866,67 nmol/10<sup>6</sup> cells) which is linked with a very high lactate production yield (2061,90 nmol/10<sup>6</sup> cells). This type of glucose overflow metabolism is typical of high glucose concentration in the media, which is indeed the case in the experiments described by Duarte et al.<sup>77</sup>, where the cell culture was initially fed with 50mM of glucose. The high lactate production can be prevented with a low and steady feed of glucose as shown by Fan Y et al.<sup>78</sup> Very likely, if these experiments were repeated with low glucose concentrations, the glucose and lactate data would likely be concordant with the theoretical fooprint.

To compare the arithmetic and weighted averaging methods, the Mean-Square-Error (MSE) between theoretical and experimental footprints were computed. The glucose and lactate data were considered outliers in the computation of the MSE. The results are shown in Table 7.

Table 7 MSE between measured and theoretical footprint

METHOD	MSE
ARITHMETIC FOOTPRINT	9.0320e+03
WEIGHTED FOOTPRINT	8.7426e+03

Although the weighted average method presented a lower MSE then the arithmetic method, the difference is not very significative. Comparing the arithmetic footprint with the weighted fooprint we can see that the differences between the footprints obtained by both methods are not significative. This could suggest a low variance in the  $\Delta G^0_r$  values of EMs. Fig 14 displays the computed  $\Delta G^0_r$  distribution, which is clearly a non-uniform distribution. This distribution has a mean value of -4.0756e-04 kJ/nmol and a variance coefficient of 73,29% which is very significant. It is not possible with these results to make a final conclusion on which method is better to compute the footprint given the small differences obtained. It is also important to mention that in simplifying the metabolic network we also influenced the  $\Delta G^0_r$  distribution of the EM. More studies are required in the future before a final conclusion can be taken.

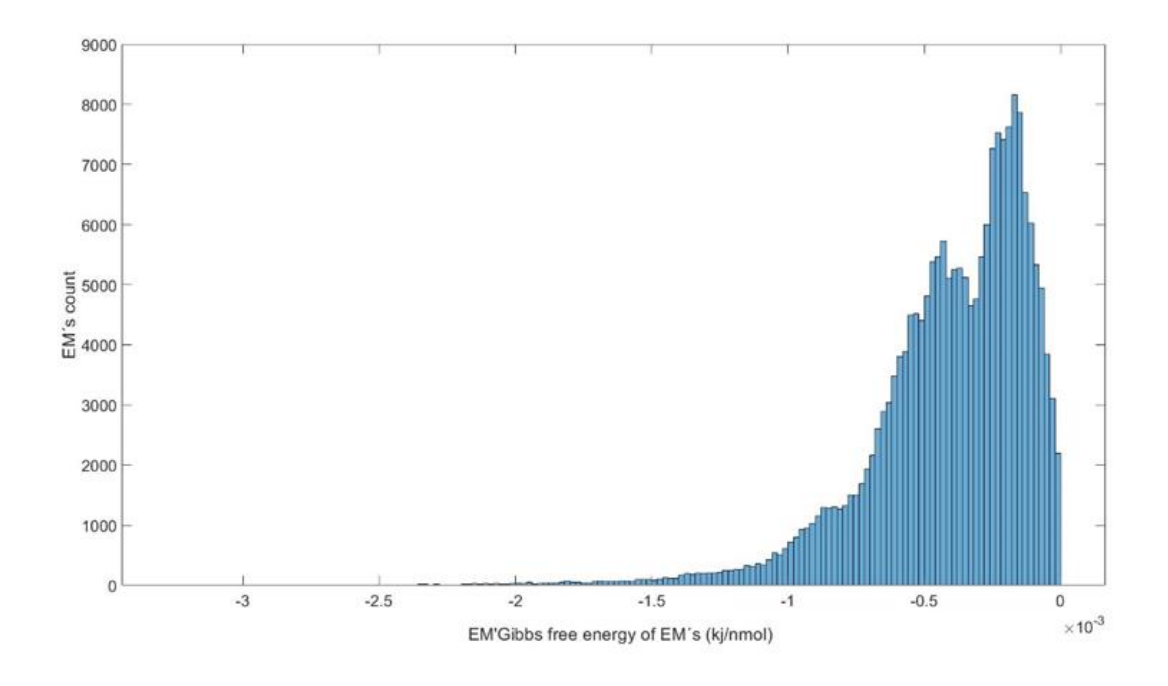


Figure 13 - Histogram  $\Delta G^{0}_{r}$  of each EM for the biomass producing network after the thermodynamic reduction step (Fig. 11)

# 3.4. Phenotype-targeted culture media design

The objective in this section is to design *In silico* culture media formulations that are targeted to a given desired phenotype. In here the following phenotypic optimal criteria were chosen

- Minimization of lactate accumulation
- Minimization of ammonium accumulation
- Minimization of osmolarity build-up
- Minimization of CO2 production

The methodology adopted is to further reduce the *footprintome* by eliminating undesired footprints that do not comply with the above enumerated criteria.

## 3.4.1 Minimization of lactate and ammonium buildup

Lactate and ammonium are by products that when accumulated to high concentrations in the media are toxic to mammalian cells. Lactate production is the by-product of an inefficient catabolism, as it only produces 2 ATP molecules compared to the 36 ATP molecules that result from the full oxidation of glucose in the TCA cycle. Lactate also acidifies the media and causes high osmolarity<sup>79</sup>, which reduces specific growth rate<sup>80</sup> and protein yield<sup>81</sup>. High ammonium concentration in the media has also a detrimental effect on the cell culture, also reducing specific growth<sup>80</sup> and protein yield<sup>82</sup>. It is therefore of high interest to design culture media formulations that minimize the accumulation of lactate and ammonium in the media.

Taking a closer look to the reduced *footprintome* for biomass production (Fig. 12) and for IgG production (Appendix F, Fig. F.2), we observe that they contain a high number of footprints that produce either lactate, ammonium or both metabolites simultaneously. In order to design a culture media that theoretically eliminates the accumulation of lactate and ammonium in the media, a phenotype targeted *footprintome* reduction is applied by removing all footprints that produce lactate and/or ammonium, as follows:

- For the biomass producing network, of the 3488 footprints present in the in the *footprintome* of Fig. 12, 1549 footprints either produce lactate and/or ammonium, and were therefore removed. The footprint count after this step is 1939.
- For the IgG producing network, of the 4704 footprints present in the *footprintome* of Appendix F (Fig. F.2), 1804 footprints produce lactate and/or ammonium and were therefore removed. The footprints count after this step is 2900.

Fig. 15 represents the biomass producing *footprintome* after the elimination of the lactate and/or ammonia producing EMs.

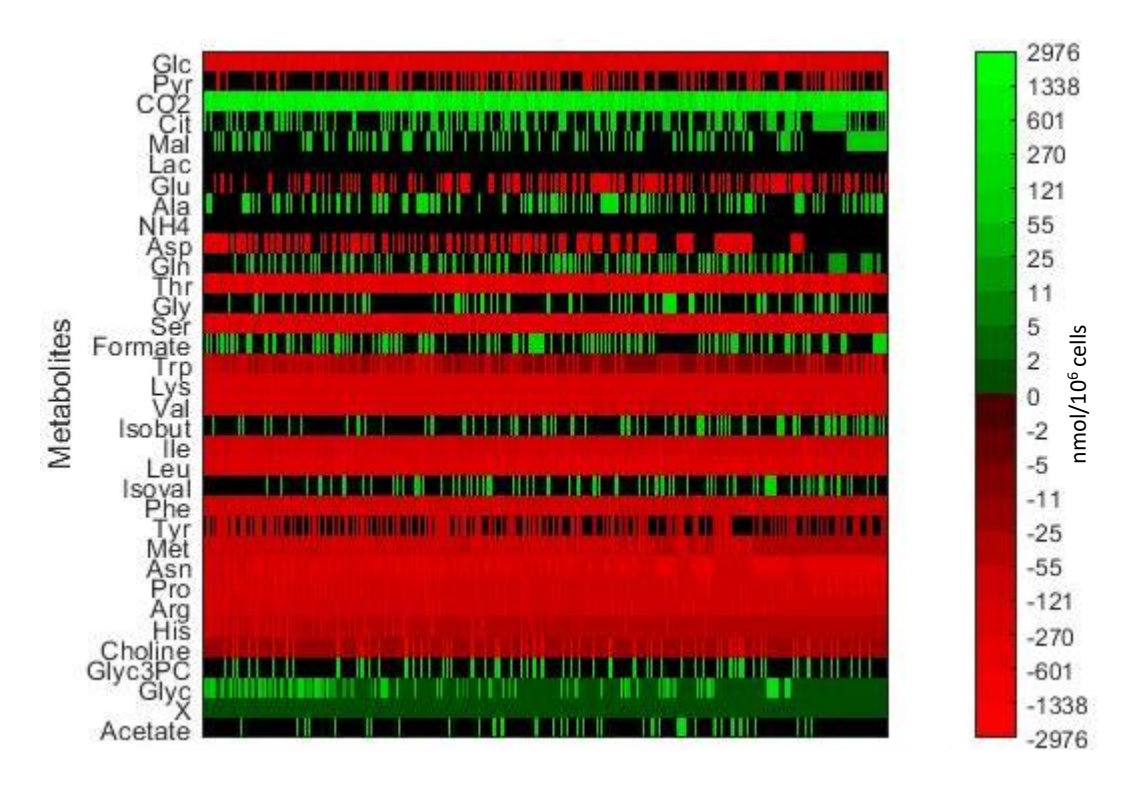


Figure 14 - Reduced footprintome for biomass production (normalized to unit) after 4 steps of reduction: Step 1- biomass production, Step 2-Thermodynamic reduction, Step 3-Pattern clustering with arithmetic averaging, Step 4- Elimination of all footprints that either produce lactate or ammonium. The rows represent extracellular media components. The columns represent average EM clusters (1939). The green gradient represents compound production associated with the production of 1 biomass unit. The red gradient represents compound consumption to generate 1 biomass unit. The black colour means that the compound is neither consumed nor produced by the EM cluster.

## 3.4.2 Minimization of osmolarity buildup

The next criteria considered are the osmolarity and CO2 of each footprint. In the study by Marie M. Zhu et.al<sup>83</sup> it is shown that osmolarity and partial pressure of CO2 have a very significant impact in a large scale CHO cell culture. High osmolarity in the culture media is shown to have a negative effect on specific growth rate and viable cell density. Moreover, it causes a shift in CHO cells metabolism leading to an increased production of lactate and ammonia. Furthermore, the combined effects of high partial pressure of CO2 (pCO2) and high osmolarity caused a more prominent effect on viable cell density than just high osmolarity alone.

The osmolarity build-up associated with each footprint was computed. The osmolarity value of a footprint was approximated by the absolute sum of metabolite values (Eq.31). As we are dealing with metabolite yields and we lack any sense of volume, these osmolarity values don't describe the real culture formula osmolarity. They can be however objectively compared between each other.

$$\sum_{i}^{n} abs(footprint_{i})$$
 (31)

Where n is the total number of metabolites in a footprint and abs(footprint<sub>i</sub>) is the absolute value of a metabolite i.

For the minimization of the osmolarity and CO2 criteria footprints associated with low osmolarity build-up and low CO2 production were selected. For this purpose, a score value (Score<sub>i</sub>) is computed for each footprint {i} according to the Eq. 32:

$$Score_{i} = \frac{Osm_{i}}{\max(Osm)} + \frac{CO2_{i}}{\max(CO2)}$$
(32)

Where,  $Osm_i$  is the osmolarity build-up associated with footprint {i}, Osm is a vector containing the osmolarity values of all footprints,  $CO2_i$  is the CO2 production by footprint {i} and CO2 is a vector containing the CO2 values of all footprints. The EM with the lowest score is the one chosen for culture media design. Figs. 16-17 show the final optimal footprint with the lowest score, for the biomass producing network (Fig. 16) and IgG producing network (Fig. 17) in comparison with their respective arithmetic footprints representatives of the *footprintome* (Fig. 13).

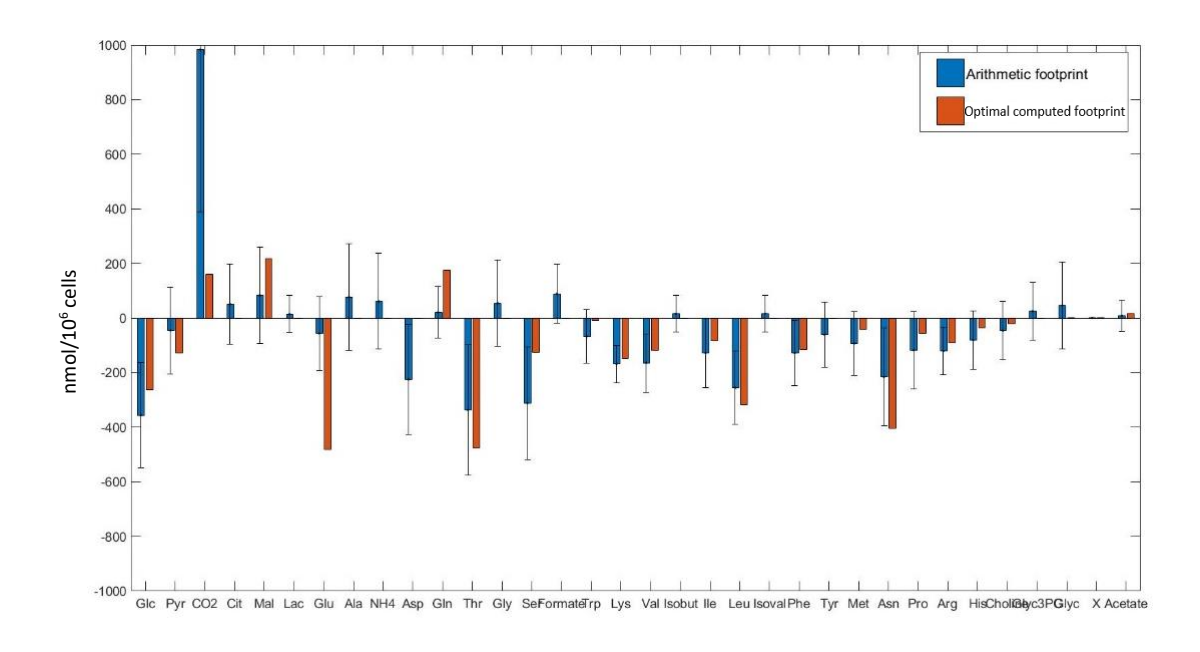


Figure 15 - Comparison between the optimal EM (orange bars) computed for the biomass producing network and the respective arithmetic footprint (blue bars).

By comparing the optimal EM with the respective arithmetic footprint (Fig. 16, for biomass production), it becomes evident the absence of lactate and ammonium production, as expected. The same can be observed for the IgG producing network (Fig.17).

In term of substrate comsumption, Fig. 16 shows that by minimizing osmolarity some substrates have a lower yield (lysine, valine, proline, histidine etc.) compared with the arithmetic footprint while others aren't consumed at all. The most prominent case is the metabolite aspartate, where in the optimal EM no consumption is predicted whereas its consumption yield is 224,78 nmol/10<sup>6</sup> cells for the arithmetic footprint. The main differences in substrate consumption are the lower glucose consumption of 263,06 nmol/10<sup>6</sup> cells compared to 356,20 nmol/10<sup>6</sup> cells, a higher glutamate consumption, 482,09 nmol/10<sup>6</sup> cells in comparison with 56,52 nmol/10<sup>6</sup> cells, an also higher consumption of asparagine 404,50 nmol/10<sup>6</sup> cells compared with 215,80 nmol/10<sup>6</sup> cells and a lower consumption of serine ,125,01 nmol/10<sup>6</sup> cells while the arithmetic footprint being 312,07 nmol/10<sup>6</sup> cells.

It may also be observed a lack of by-products formation in the optimal EM. Examples of this are the, isobut, isoval, alanine, glycine and formate. On the contrary, malate and glutamine are increased. Also the CO2 production is much lower in the formula chosen as a result of minimizing CO2 production, being 161,46 nmol/10<sup>6</sup> cells compared to the arithmetic footprint of 983,73 nmol/10<sup>6</sup> cells. The full list of results can be found in Appendix E, Table E.1

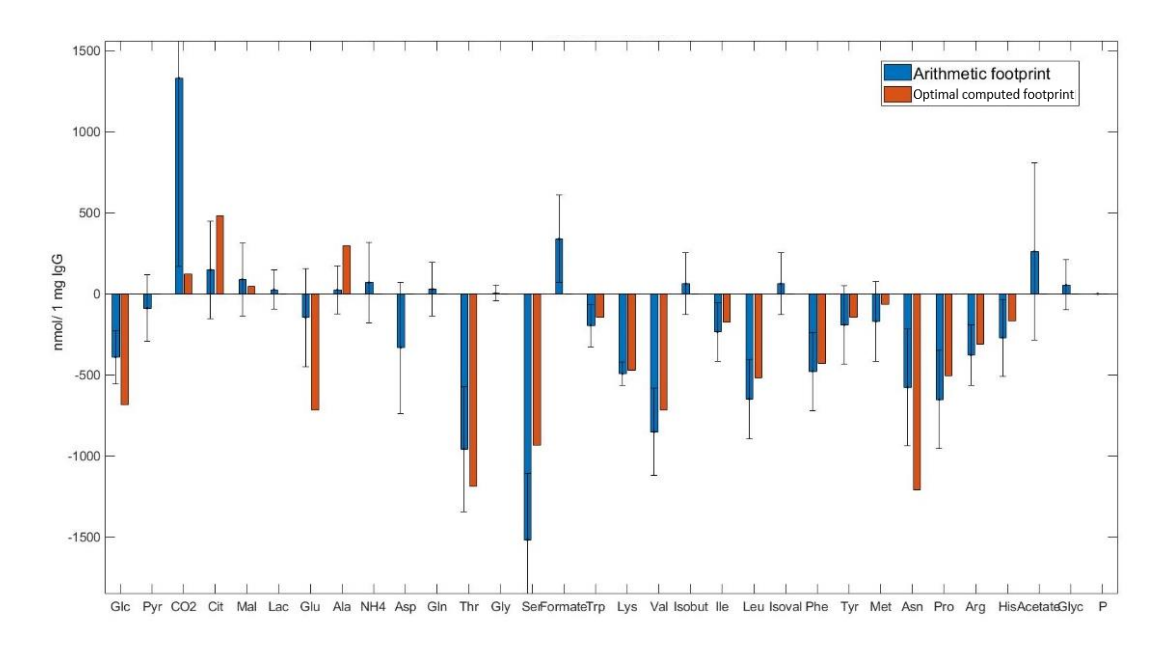


Figure 16 - Comparison between the optimal EM computed (orange bars) for the IgG producing network and the respective arithmetic footprint (blue bars).

The effects of minimizing osmolarity and CO2 had similar results for the product producing network, with substrates having lower consumption (lysine, valine, proline, histidine etc.), the non-consumption of aspartate and lack of by-product formation (isobut, isoval, glycine, formate) and an increase in specific by-products productions (citrate and alanine). The CO2 production also dropped sharply compared with the arithmetic footprint from 1330,80 nmol/10<sup>6</sup> cells to 120,92 nmol/10<sup>6</sup> cells, interestingly the glucose has a higher consumption yield in the optimal EM with 681,53 nmol/10<sup>6</sup> cells compared with 390,55 nmol/10<sup>6</sup> cells. The glutamate, serine and asparagine yields show similar behaviour to the biomass optimal EM. It should however be noted that the amount of glucose used for IgG production should be much less than that for biomass production. The full list of results can be found in Appendix E, Table E.2

#### 3.4.3 Final culture media concentrations

In order to formulate the final optimal culture media composition, the concentrations of each compound need to be specified. The footprints are not ready to be used as culture media formulas because they are expressed as yields. As such, they need to be multiplied by a concentration value of the target product (Eq.30).

The concentration used for the optimal IgG producing EM was 0.56 mg of IgG/ml, this being the mean value of the results from the work of Reinhart, D, et. al.  $^{84}$  where they benchmarked several commercial CHO culture medias for IgG antibody production, measuring the IgG concentration in all tested medias.

The concentrations for the optimal biomass producing EM were obtained by initially multiplying the computed formula by a cell concentration of 10 10<sup>6</sup> cell/ml the formula. It was then compared with a lab tested CHO culture media. The cell concentration was adjusted such as to minimize the MSE between the computed and experimental concentrations. The final cell concentration calculated was 17,55 10<sup>6</sup> cell/ml (still in reasonable range) for a MSE value of 42,88.

The comparison between lab tested CHO culture media with the final computed formula for biomass synthesis is shown in Fig 18, these results are also shown in Table 8 alongside the computed formula for IgG synthesis.

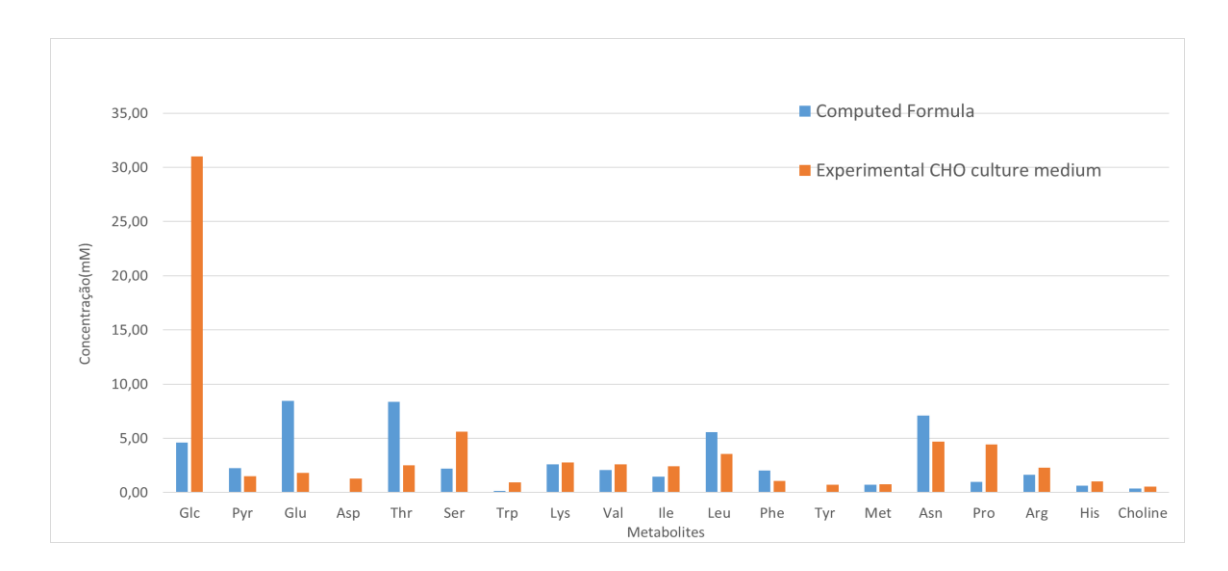


Figure 17 - Comparison between the computed formula for biomass synthesis (blue bars) with experimental CHO culture media (orange bars).

Fig.18 shows many similarities between the *In silico* formula for biomass synthesis (blue bars) and the lab tested CHO culture media (orange bars). The metabolites with more concordant concentrations (between *In silico* and experiment) were lysine, valine, histidine, arginine and choline. A significant difference is observed for glutamate and threonine concentrations, with higher *In silico* concentrations (8,46 mM and 8,35 mM respectively) than the experimental concentrations (1,79 mM and 2,50 mM respectively). The largest mismatch is a much lower *In silico* glucose concentration (4,62 mM) than the experimental concentration (31,01 mM). Glucose is the preferred carbon source by CHO cells. In batch runs, high amounts of glucose are usually formulated in the culture media. A lower glucose concentration in the *In silico* formula suggests that it needs to be complemented with a continuous feeding strategy of glucose.

 $\begin{tabular}{ll} Table~8~Computed~formulas~for~IgG~and~biomass~syntheses~and~Lab~tested~CHO~culture~media \end{tabular}$ 

Metabolites	Computed formula for IgG synthesis (mM)	Computed formula for biomass synthesis (mM)	Lab tested CHO culture media (mM)
$\overline{Glc}$	0,38	4,62	31,01
Pyr	0,00	2,23	1,52
Glu	0,40	8,46	1,79
Asp	0,00	0,00	1,29
Thr	0,66	8,35	2,50
Ser	0,52	2,19	5,60
Trp	0,08	0,16	0,93
Lys	0,26	2,59	2,78
Val	0,40	2,08	2,58
Ile	0,10	1,45	2,41
Leu	0,29	5,57	3,54
Phe	0,24	2,02	1,05
Tyr	0,08	0,00	0,70
Met	0,04	0,70	0,74
Asn	0,67	7,10	4,71
Pro	0,28	0,97	4,42
Arg	0,17	1,61	2,28
His	0,09	0,64	1,00
Choline	-	0,37	0,52

# 4. Conclusions

In this work a method was developed capable of computing culture media *In silico* using only a metabolic network of a target cell line as input and elementary mode analysis (EMA). The Chinese Hamster Ovary (CHO) metabolic network was used as a case-study in order to validate our approach. The proposed tool is an alternative to empirical and wet lab intensive methods used in the industry, like RSM.

The main challenge in using EMA for *In silico* culture media design, is the elementary mode computation combinatorial explosion, the computational burden associated with computing all EM in the case study CHO metabolic network was too high. As a result, we used a more simplistic CHO metabolic network without the respective oxidative phosphorylation reactions, closing the balances for carbon and nitrogen but not for oxygen and hydrogen, which is suboptimal. We want the computed footprints values displayed in the *footprintome* to be as representative of the different metabolisms of the targeted cell line as possible, the more complete the metabolic network in use is the better, a genome scale network would be ideal but it's not feasible due to the computation power needed to calculate all possible millions of EMs in a network of this scale.

Even with these drawbacks this study obtained optimistic results:

- The arithmetic and the weighted footprints when compared with the footprints calculated from the experimental literature data<sup>77</sup> (Fig. 13A), shows that the majority of metabolite yields values in the literature data, are on the variance bounds of the theoretical footprints computed (21 out of the 26 metabolites). Which indicates that a general predictions of the metabolism footprint of a target cell line can be done using this method
- The phenotype target design has shown to be a useful method for selecting optimal metabolic footprints, the differences between the optimal computed EMs for both networks and the arithmetic footprints of the respective networks were concordant with the selective criteria chosen.
- The similarities observed between the optimal EM for the biomass producing network with a lab teste CHO culture media (MSE value of 42,88 for a cell concentration of 17,55 10<sup>6</sup> cell/ml), shown that this tool is capable of computing reasonable culture media formulas that can be further tested in the lab.

The present M.Sc. thesis had the objective to develop a method in MATLAB capable of computing culture media *In silico* using only the targeted cell line metabolic network, this objective was reached, the positive results shown that further studies regarding the usage and development of the methods present in this thesis are worth pursuing.

#### 4.1 Future work

The arithmetic and the weighted footprint shown similar results when compared with the data published by Duarte et. al. 77, as already discussed, but we could not conclude which of these methods is better and further research is needed. This methodology should be tested with different cell lines metabolic networks and the results compared with available literature data, to better understand the difference between the two methods and to confirm if the results observed in this thesis are also true for different cell lines.

There are several options for future work regarding the phenotype-targeted culture media phase:

- The culture media for growth and IgG production computed in this thesis, should be teste in the lab to quantify the differences between the computed formulas and the experimental results, to study if the computed culture medias can have a decisive effect in controlling the active EMs of the CHO cell metabolism.
- Different culture media formulas should be computed using different criteria (e. g. minimization of glucose consumption) to study which criteria or combination of criteria can be used to better match the experimental results, the number of criteria used can also be a decisive factor.
- Different metabolic networks can be tested to understand more the potential of the toolbox and to further develop it.

# 5. References

- 1. Plackett RL and Burman J. P. THE DESIGN OF OPTIMUM MULTIFACTORIAL EXPERIMENTS Design of optimum multifactorial experiments. *Biometrika*. 1946;33(4):305-325.
- 2. Box AGEP, Wilson KB, Journal S, Statistical R, Series S. On the Experimental Attainment of Optimum Conditions Published by: Wiley for the Royal Statistical Society Stable URL: http://www.jstor.org/stable/2983966. 1951;13(1):1-45.
- 3. Taguchi G, Rafanelli AJ. *Taguchi on Robust Technology Development: Bringing Quality Engineering Upstream.* Vol 116.; 1992. doi:10.1115/1.2905506
- 4. McCulloch WS, Pitts W. A logical calculus of the ideas immanent in nervous activity. *Bull Math Biophys.* 1943;5(4):115-133. doi:10.1007/BF02478259
- 5. Glassey J, Montague GA, Ward AC, Kara B V. Artificial neural network based experimental design procedure for enhancing fermentation development. *Biotechnol Bioeng*. 1994;44(4):397-405. doi:10.1002/bit.260440402
- 6. Mitchell M (Computer scientist). *An Introduction to Genetic Algorithms*. MIT Press; 1996.
- 7. Weuster-Botz D, Wandrey C. Medium Optimization by Genetic Algorithm for Continuous Production of Formate Dehydrogenase. *Process Biochem.* 1995;30(6):563-571. doi:10.1016/0032-9592(94)00036-0
- 8. Stephanopoulos G. Metabolic Fluxes and Metabolic Engineering. *Metab Eng*. 1999;1(1):1-11. doi:10.1006/mben.1998.0101
- 9. Reder C. Metabolic control theory: A structural approach. *J Theor Biol*. 1988;135(2):175-201. doi:10.1016/S0022-5193(88)80073-0
- 10. Stephanopoulos G, Aristidou AA NJ. *Metabolic Engineering PRINCIPLES AND METHODOLOGIES*. (Academic SD, ed.).; 1998.
- 11. Kauffman KJ, Prakash P, Edwards JS. Advances in flux balance analysis. *Curr Opin Biotechnol*. 2003;14(5):491-496. doi:10.1016/j.copbio.2003.08.001
- 12. SCHUSTER, S., & HILGETAG C. ON ELEMENTARY FLUX MODES IN BIOCHEMICAL REACTION SYSTEMS AT STEADY STATE. *J Biol Syst*. 1994;02(02):165-182.
- 13. Im JH, Song JM, Kang JH, Kang DJ. Optimization of medium components for high-molecular-weight hyaluronic acid production by Streptococcus sp. ID9102 via a statistical approach. *J Ind Microbiol Biotechnol*. 2009;36(11):1337-1344. doi:10.1007/s10295-009-0618-8
- 14. Behera HT, Upadhyay AK, Raina V, Ray L. Optimization of media components for the production of N-acetylchitooligosaccharide from chitin by Streptomyces chilikensis through Taguchi experimental design. *J Microbiol Methods*. 2019;159(February):194-199. doi:10.1016/j.mimet.2019.03.014
- 15. Darvishi F, Moghaddami NA. Optimization of an industrial medium from molasses for bioethanol production using the Taguchi statistical experimental-design method. *Fermentation*. 2019;5(1). doi:10.3390/fermentation5010014
- 16. Khanna S, Ranjan A, Goyal A, Moholkar VS. Medium optimization for mixed alcohols

- production by glycerol utilizing immobilized Clostridium pasteurianum MTCC 116. *Chem Biochem Eng Q.* 2013;27(3):319-325.
- 17. Mehta PK, Bhatia SK, Bhatia RK, Bhalla TC. Enhanced production of thermostable amidase from Geobacillus subterraneus RL-2a MTCC 11502 via optimization of physicochemical parameters using Taguchi DOE methodology. *3 Biotech*. 2016;6(1):1-12. doi:10.1007/s13205-016-0390-1
- 18. Rajendran A, Thirugnanam M, Thangavelu V. Statistical evaluation of medium components by Plackett-Burman experimental design and kinetic modeling of lipase production by Pseudomonas fluorescens. *Indian J Biotechnol*. 2007;6(4):469-478.
- 19. Ashengroph M, Nahvi I, Amini J. Application of taguchi design and response surface methodology for improving conversion of isoeugenol into vanillin by resting cells of Psychrobacter sp. CSW4. *Iran J Pharm Res.* 2013;12(3):411-421. doi:10.22037/ijpr.2013.1337
- 20. Teng Y, Xu Y. Culture condition improvement for whole-cell lipase production in submerged fermentation by Rhizopus chinensis using statistical method. *Bioresour Technol*. 2008;99(9):3900-3907. doi:10.1016/j.biortech.2007.07.057
- 21. Hanchinal VM, Survase SA, Sawant SK, Annapure US. Response surface methodology in media optimization for production of β-carotene from Daucus carota. *Plant Cell Tissue Organ Cult*. 2008;93(2):123-132. doi:10.1007/s11240-008-9350-8
- 22. Isiaka Adetunji A, Olufolahan Olaniran A. Optimization of culture conditions for enhanced lipase production by an indigenous Bacillus aryabhattai SE3-PB using response surface methodology. *Biotechnol Biotechnol Equip*. 2018;32(6):1514-1526. doi:10.1080/13102818.2018.1514985
- Chen L, Alcazar J, Yang T, Lu Z, Lu Y. Optimized cultural conditions of functional yogurt for γ-aminobutyric acid augmentation using response surface methodology. *J Dairy Sci.* 2018;101(12):10685-10693. doi:10.3168/jds.2018-15391
- 24. Ekpenyong MG, Antai SP, Asitok AD, Ekpo BO. Plackett-burman design and response surface optimization of medium trace nutrients for glycolipopeptide biosurfactant production. *Iran Biomed J.* 2017;21(4):249-260. doi:10.18869/acadpub.ibj.21.4.249
- 25. Cui JD, Jia SR. Optimization of medium on exopolysaccharides production in submerged culture of Cordyceps militaris. *Food Sci Biotechnol*. 2010;19(6):1567-1571. doi:10.1007/s10068-010-0222-8
- 26. Marteijn RCL, Jurrius O, Dhont J, De Gooijer CD, Tramper J, Martens DE. Optimization of a feed medium for fed-batch culture of insect cells using a genetic algorithm. *Biotechnol Bioeng*. 2003;81(3):269-278. doi:10.1002/bit.10465
- 27. Etschmann MMW, Sell D, Schrader J. Medium optimization for the production of the aroma compound 2-phenylethanol using a genetic algorithm. *J Mol Catal B Enzym*. 2004;29(1-6):187-193. doi:10.1016/j.molcatb.2003.10.014
- 28. Camacho-Rodríguez J, Cerón-García MC, Fernández-Sevilla JM, Molina-Grima E. Genetic algorithm for the medium optimization of the microalga Nannochloropsis gaditana cultured to aquaculture. *Bioresour Technol*. 2015;177:102-109. doi:10.1016/j.biortech.2014.11.057
- 29. García-Camacho F, Gallardo-Rodríguez JJ, Sánchez-Mirón A, Chisti Y, Molina-Grima E. Genetic algorithm-based medium optimization for a toxic dinoflagellate microalga. *Harmful Algae*. 2011;10(6):697-701. doi:10.1016/j.hal.2011.05.005
- 30. Siddique S, Nelofer R, Syed Q, Adnan A, Qureshi FA. Optimization for the enhanced

- production of avermectin B1b from Streptomyces avermitilis DSM 41445 using artificial neural network. *J Korean Soc Appl Biol Chem.* 2014;57(5):677-683. doi:10.1007/s13765-014-4194-x
- 31. Pathak L, Singh V, Niwas R, et al. Artificial intelligence versus statistical modeling and optimization of cholesterol oxidase production by using Streptomyces sp. *PLoS One*. 2015;10(9):1-14. doi:10.1371/journal.pone.0137268
- 32. Haider MA, Pakshirajan K, Singh A, Chaudhry S. Artificial neural network-genetic algorithm approach to optimize media constituents for enhancing lipase production by a soil microorganism. *Appl Biochem Biotechnol*. 2008;144(3):225-235. doi:10.1007/s12010-007-8017-y
- 33. H.A. Shakir, R. Mahmood, M. Irfan, F. Deeba, I. Javed JIQ. PROTEASE PRODUCTION FROM Bacillus safensis IN SUBMERGED FERMENTATION USING RESPONSE SURFACE METHODOLOGY. *Rev Mex Ing Química*. 2019;18(1):375-385.
- 34. Makowski K, Matusiak K, Borowski S, et al. Optimization of a culture medium using the Taguchi approach for the production of microorganisms active in odorous compound removal. *Appl Sci.* 2017;7(8). doi:10.3390/app7080756
- 35. Response Surface Methods for Optimization ReliaWiki. http://reliawiki.org/index.php/Response\_Surface\_Methods\_for\_Optimization. Accessed January 21, 2020.
- 36. Morowvat MH, Ghasemi Y. Culture medium optimization for enhanced β-carotene and biomass production by Dunaliella salina in mixotrophic culture. *Biocatal Agric Biotechnol*. 2016;7:217-223. doi:10.1016/j.bcab.2016.06.008
- Kovárová-Kovar K, Egli T. Growth kinetics of suspended microbial cells: from single-substrate-controlled growth to mixed-substrate kinetics. *Microbiol Mol Biol Rev*. 1998;62(3):646-666.
   http://www.ncbi.nlm.nih.gov/pubmed/9729604%0Ahttp://www.pubmedcentral.nih.gov/articlerender.fcgi?artid=PMC98929.
- 38. Hajmeer MN, Basheer IA, Najjar YM. Computational neural networks for predictive microbiology II. Application to microbial growth. *Int J Food Microbiol*. 1997;34(1):51-66. doi:10.1016/S0168-1605(96)01169-5
- 39. A general model of a deep neural network. It consists of an input... | Download Scientific Diagram. https://www.researchgate.net/figure/A-general-model-of-a-deep-neural-network-It-consists-of-an-input-layer-some-here-two\_fig1\_308414212. Accessed June 26, 2020.
- 40. Smaoui S, Ennouri K, Chakchouk-Mtibaa A, et al. Statistical versus artificial intelligence -based modeling for the optimization of antifungal activity against Fusarium oxysporum using Streptomyces sp. strain TN71. *J Mycol Med.* 2018;28(3):551-560. doi:10.1016/j.mycmed.2018.07.003
- 41. Rafigh SM, Yazdi AV, Vossoughi M, Safekordi AA, Ardjmand M. Optimization of culture medium and modeling of curdlan production from Paenibacillus polymyxa by RSM and ANN. *Int J Biol Macromol*. 2014;70:463-473. doi:10.1016/j.ijbiomac.2014.07.034
- 42. Talib NSR, Halmi MIE, Ghani SSA, Zaidan UH, Shukor MYA. Artificial Neural Networks (ANNs) and Response Surface Methodology (RSM) Approach for Modelling the Optimization of Chromium (VI) Reduction by Newly Isolated Acinetobacter radioresistens Strain NS-MIE from Agricultural Soil. *Biomed Res Int.* 2019;2019.

- doi:10.1155/2019/5785387
- 43. Understanding the Genetic Algorithm Noteworthy The Journal Blog. https://blog.usejournal.com/understanding-the-genetic-algorithm-4eac04a07a59. Accessed April 10, 2020.
- 44. Genetic Algorithms Definition | DeepAI. https://deepai.org/machine-learning-glossary-and-terms/genetic-algorithms. Accessed January 24, 2020.
- 45. Özer A, Gürbüz G, Çalimli A, Körbahti BK. Biosorption of copper(II) ions on Enteromorpha prolifera: Application of response surface methodology (RSM). *Chem Eng J.* 2009;146(3):377-387. doi:10.1016/j.cej.2008.06.041
- 46. Tortajada M, Llaneras F, Picó J. 2010 Tortajada, Llaneras, Picó BMC systems biology.pdf. 2010.
- 47. Provost A, Bastin G, Agathos SN, Schneider YJ. Metabolic design of macroscopic bioreaction models: Application to Chinese hamster ovary cells. *Bioprocess Biosyst Eng.* 2006;29(5-6):349-366. doi:10.1007/s00449-006-0083-y
- 48. Noda S, Mori Y, Oyama S, Kondo A, Araki M, Shirai T. Reconstruction of metabolic pathway for isobutanol production in Escherichia coli. *Microb Cell Fact*. 2019;18(1):124. doi:10.1186/s12934-019-1171-4
- 49. BiGG Models. http://bigg.ucsd.edu/. Accessed April 10, 2020.
- 50. Trinh CT, Wlaschin A, Srienc F. Elementary mode analysis: A useful metabolic pathway analysis tool for characterizing cellular metabolism. *Appl Microbiol Biotechnol*. 2009;81(5):813-826. doi:10.1007/s00253-008-1770-1
- 51. Gregoty N. Stephanopoulos, Aristos A. Aristidou JN. *Metabolic Engineering: Princeples and Methdologies.*; 1998.
- 52. Wilkens CA, Altamirano C, Gerdtzen ZP. Comparative metabolic analysis of lactate for CHO cells in glucose and galactose. *Biotechnol Bioprocess Eng.* 2011;16(4):714-724. doi:10.1007/s12257-010-0409-0
- 53. Xing Z, Kenty B, Koyrakh I, Borys M, Pan SH, Li ZJ. Optimizing amino acid composition of CHO cell culture media for a fusion protein production. *Process Biochem.* 2011;46(7):1423-1429. doi:10.1016/j.procbio.2011.03.014
- 54. McAtee Pereira AG, Walther JL, Hollenbach M, Young JD. 13C Flux Analysis Reveals that Rebalancing Medium Amino Acid Composition can Reduce Ammonia Production while Preserving Central Carbon Metabolism of CHO Cell Cultures. *Biotechnol J*. 2018;13(10):1-7. doi:10.1002/biot.201700518
- 55. Schuetz R, Kuepfer L, Sauer U. Systematic evaluation of objective functions for predicting intracellular fluxes in Escherichia coli. *Mol Syst Biol*. 2007;3(119). doi:10.1038/msb4100162
- Costa RS, Nguyen S, Hartmann A, Vinga S. Exploring the cellular objective in flux balance constraint-based models. *Lect Notes Comput Sci (including Subser Lect Notes Artif Intell Lect Notes Bioinformatics)*. 2014;8859:211-224. doi:10.1007/978-3-319-12982-2\_15
- 57. Chen Y, Dong F, Wang Y. Systematic development and optimization of chemically defined medium supporting high cell density growth of Bacillus coagulans. *Appl Microbiol Biotechnol*. 2016;100(18):8121-8134. doi:10.1007/s00253-016-7644-z
- 58. Rockafellar R. Book Convex analysis. *Princet Univ Press*. 1997.

- 59. Çakir T, Kirdar B, Önsan ZI, Ülgen KÖ, Nielsen J. Effect of carbon source perturbations on transcriptional regulation of metabolic fluxes in Saccharomyces cerevisiae. *BMC Syst Biol.* 2007;1:1-10. doi:10.1186/1752-0509-1-18
- 60. R2019a Updates to the MATLAB and Simulink product families MATLAB & Simulink. https://www.mathworks.com/products/new\_products/release2019a.html. Accessed April 10, 2020.
- 61. Terzer M, Stelling J. Accelerating the computation of elementary modes using pattern trees. *Lect Notes Comput Sci (including Subser Lect Notes Artif Intell Lect Notes Bioinformatics)*. 2006;4175 LNBI(1):333-343. doi:10.1007/11851561 31
- 62. Klamt S, Stelling J. Combinatorial complexity of pathway analysis in metabolic networks. *Mol Biol Rep.* 2002;29(1-2):233-236. doi:10.1023/A:1020390132244
- 63. Stephanopoulos GN, Aristidou AA, Nielsen J. Thermodynamics of Cellular Processes. *Metab Eng.* 1998:629-694. doi:10.1016/b978-012666260-3/50015-7
- 64. Gibbs (Free) Energy Chemistry LibreTexts.
  https://chem.libretexts.org/Bookshelves/Physical\_and\_Theoretical\_Chemistry\_Textbook
  \_Maps/Supplemental\_Modules\_(Physical\_and\_Theoretical\_Chemistry)/Thermodynamic
  s/Energies\_and\_Potentials/Free\_Energy/Gibbs\_(Free)\_Energy. Accessed February 13,
  2020.
- 65. eQuilibrator: The Biochemical Thermodynamics Calculator. http://equilibrator.weizmann.ac.il/. Accessed February 15, 2020.
- 66. Noor E, Haraldsdóttir HS, Milo R, Fleming RMT. Consistent Estimation of Gibbs Energy Using Component Contributions. *PLoS Comput Biol*. 2013;9(7). doi:10.1371/journal.pcbi.1003098
- 67. Laux H. Industry perspective on Chinese hamster ovary cell "omics" SPECIAL FOCUS y An 'omics approach to Chinese hamster ovary-based pharmaceutical bioprocessing. *Pharm Bioprocess*. 2014;2(5):377-381. doi:10.4155/PBP.14.48
- 68. Carinhas N, Duarte TM, Barreiro LC, Carrondo MJT, Alves PM, Teixeira AP. Metabolic signatures of GS-CHO cell clones associated with butyrate treatment and culture phase transition. *Biotechnol Bioeng*. 2013;110(12):3244-3257. doi:10.1002/bit.24983
- 69. Quek LE, Dietmair S, Krömer JO, Nielsen LK. Metabolic flux analysis in mammalian cell culture. *Metab Eng.* 2010;12(2):161-171. doi:10.1016/j.ymben.2009.09.002
- 70. Sengupta N, Rose ST, Morgan JA. Metabolic flux analysis of CHO cell metabolism in the late non-growth phase. *Biotechnol Bioeng*. 2011;108(1):82-92. doi:10.1002/bit.22890
- 71. Zamorano F, Wouwer A Vande, Bastin G. A detailed metabolic flux analysis of an underdetermined network of CHO cells. *J Biotechnol*. 2010;150(4):497-508. doi:10.1016/j.jbiotec.2010.09.944
- 72. efmtool Computational Systems Biology | ETH Zurich. https://csb.ethz.ch/tools/software/efmtool.html. Accessed April 14, 2020.
- 73. Schuster S, Dandekar T, Fell DA. Detection of elementary flux modes in biochemical networks: A promising tool for pathway analysis and metabolic engineering. *Trends Biotechnol.* 1999;17(2):53-60. doi:10.1016/S0167-7799(98)01290-6
- 74. Song HS, Ramkrishna D. Reduction of a set of elementary modes using yield analysis. *Biotechnol Bioeng*. 2009;102(2):554-568. doi:10.1002/bit.22062
- 75. Folch-Fortuny A, Marques R, Isidro IA, Oliveira R, Ferrer A. Principal elementary mode analysis (PEMA). *Mol Biosyst.* 2016;12(3):737-746. doi:10.1039/c5mb00828j

- 76. Ferreira AR, Dias JML, Teixeira AP, et al. Projection to latent pathways (PLP): A constrained projection to latent variables (PLS) method for elementary flux modes discrimination. *BMC Syst Biol*. 2011;5. doi:10.1186/1752-0509-5-181
- 77. Duarte TM, Carinhas N, Barreiro LC, Carrondo MJT, Alves PM, Teixeira AP. Metabolic responses of CHO cells to limitation of key amino acids. *Biotechnol Bioeng*. 2014;111(10):2095-2106. doi:10.1002/bit.25266
- 78. Fan Y, Jimenez Del Val I, Müller C, et al. Amino acid and glucose metabolism in fedbatch CHO cell culture affects antibody production and glycosylation. *Biotechnol Bioeng*. 2015;112(3):521-535. doi:10.1002/bit.25450
- 79. Li F, Vijayasankaran N, Shen A, Kiss R, Amanullah A. Cell culture processes for monoclonal antibody production. *MAbs*. 2010;2(5):466-479. doi:10.4161/mabs.2.5.12720
- 80. Kurano N, Leist C, Messi F, Kurano S, Fiechter A. Growth behavior of Chinese hamster ovary cells in a compact loop bioreactor. 2. Effects of medium components and waste products. *J Biotechnol*. 1990;15(1-2):113-128. doi:10.1016/0168-1656(90)90055-G
- 81. Glacken MW, Fleischaker RJ, Sinskey AJ. Reduction of waste product excretion via nutrient control: Possible strategies for maximizing product and cell yields on serum in cultures of mammalian cells. *Biotechnol Bioeng*. 1986;28(9):1376-1389. doi:10.1002/bit.260280912
- 82. Hansen HA, Emborg C. Influence of Ammonium on Growth, Metabolism, and Productivity of a Continuous Suspension Chinese Hamster Ovary Cell Culture. *Biotechnol Prog.* 1994;10(1):121-124. doi:10.1021/bp00025a014
- 83. Zhu MM, Goyal A, Rank DL, Gupta SK, Vanden Boom T, Lee SS. Effects of elevated pCO2 and osmolality on growth of CHO cells and production of antibody-fusion protein B1: A case study. *Biotechnol Prog.* 2005;21(1):70-77. doi:10.1021/bp049815s
- 84. Avid, Damjanovic L, Kaisermayer C, Kunert R. Benchmarking of commercially available CHO cell culture media for antibody production. *Appl Microbiol Biotechnol*. 2015;99(11):4645-4657. doi:10.1007/s00253-015-6514-4
- 85. Singh V, Haque S, Niwas R, Srivastava A, Pasupuleti M, Tripathi CKM. Strategies for fermentation medium optimization: An in-depth review. *Front Microbiol*. 2017;7(JAN). doi:10.3389/fmicb.2016.02087

# Appendix

# Appendix A – CHO Metabolic Networks

# Table A.1 Metabolic Network for CHO cell line

Table A.1 Metabolic Network for CHO cell line

#	Reactions
	Glicolysis
1	1 Glc + 1 ATP> 1 G6P
2	1 G6P> 1 F6P
3	1 F6P + 1 ATP> 1 GAP + 1 DHAP
4	1 DHAP> 1 GAP
5	1 GAP> 1 NADH + 1 ATP + 1 3PG
6	1 3PG> 1 Pyr + 1 ATP
	TCA cycle
7	1 Pyr> 1 CO2 + 1 AcCoA + 1 NADH
8	1 AcCoA + 1 Oxal> 1 Cit
9	1 Cit> 1 CO2 + 1 aKG + 1 NADH
10	1 aKG> 1 CO2 + 1 SucCoA + 1 NADH
11	1 SucCoA> 1 Succ + 1 ATP
12	1 Succ> 1 Fum + 1 FADH2
13	1 Fum> 1 Mal
14	1 Mal> 1 Oxal + 1 NADH
	Pyruvate fates
15	1 Pyr + 1 NADH> 1 Lac
16	1 Pyr + 1 Glu> 1 Ala + 1 aKG
	Pentose Phosphate Pathway
17	3 G6P> 3 CO2 + 3 R5P + 6 NADPH
	Anaplerotic Reaction
18	1 Mal> 1 Pyr + 1 CO2 + 1 NADPH
	Amino Acid Metabolism
19	1 Glu <> 1 aKG + 1 NH4 + 1 NADH
20	1 aKG + 1 Asp> 1 Glu + 1 Oxal
21	1 Glu + 1 NH4 + 1 ATP> Gln
22	1 Thr> 1 AcCoA + 1 Gly + 1 NADH
23	1 Ser> 1 Gly + 1 NADPH + 1 ATP + 1 Formate
24	1 Ser> 1 Pyr + 1 NH4
25	1 Thr> 1 NH4 + 1 aKb
26	1 ATP + 1 aKb> 1 SucCoA + 1 NADH
27	1 Trp> 2 CO2 + 1 Ala + 1 aKa
28	2 aKG + 1 Lys> 2 Glu + 3 NADPH + 1 FADH2 + 1 aKa
29	1 aKa> 2 CO2 + 2 AcCoA + 2 NADH
30	1 aKG + 1 Val> 1 CO2 + 1 Glu + 1 NADH + 1 IsobutCoA

31	1 ATP + 1 IsobutCoA> 1 SucCoA + 2 NADH + 1 FADH2
32	1 IsobutCoA> 1 Isobut
33	1 aKG + 1 Ile + 1 ATP> 1 Glu + 1 AcCoA + 1 SucCoA + 2 NADH + 1
	FADH2
34	1 aKG + 1 Leu> 1 CO2 + 1 Glu + 1 NADH + 1 IsovalCoA
35	1 CO2 + 1 SucCoA + 1 ATP + 1 IsovalCoA> 3 AcCoA + 1 Succ + 1 FADH2
36	1 IsovalCoA> 1 Isoval
37	1 Phe + 1 NADH> 1 Tyr
38	1 aKG + 1 SucCoA + 1 Tyr> 1 CO2 + 1 Glu + 2 AcCoA + 1 Fum + 1 Succ
39	1 Ser + 1 Met + 1 ATP> 1 NH4 + 1 aKb
40	1 Asn> 1 NH4 + 1 Asp
41	1 Pro> 1 Glu + 1 NADH
42	1 aKG + 1 Arg> 2 Glu + 1 NADH
43	1 His> 1 Glu + 1 NH4
	Glycogen Synthesis
44	1 G6P> 1 G1P
45	2 ATP + 1 G1P + 1 UMPRN> 1 UDPG
46	1 UDPG> 1 Glycogen
	Nucleotide Synthesis
47	1 R5P + 1 ATP> 1 PRPP
48	1 CO2 + 2 Gln + 1 Gly + 1 Asp + 5 ATP + 1 PRPP> 2 Glu + 1 Fum + 1 IMP
49	1 Asp + 2 ATP + 1 GMPRN + 1 IMP> 1 Fum + 1 AMPRN
50	1 Gln + 1 ATP + 1 IMP> 1 Glu + 1 NADH + 1 GMPRN
51	1 NH4 + 1 Asp + 2 ATP + 1 CO2> 1 NADH + 1 Orotate
52	1 Orotate + 1 PRPP> 1 CO2 + 1 UMPRN
53	1 Gln + 1 ATP + 1 UMPRN> 1 Glu + 1 CMPRN
54	1 AMPRN> 1 dAMP
55	1 GMPRN> 1 dGMP
56	1 CMPRN> 1 dCMP
57	1 UMPRN> 1 dTMP
	Lipid Synthesis
58	1 ATP + 1 Choline> 1 Pcholine
59	18 AcCoA + 33 NADH + 22 ATP + 1 Glyc3P + 1 Pcholine> 1 PC
60	1 Ser + 1 PC> 1 PS + 1 Choline
61	1 PS> 1 CO2 + 1 PE
62	1 Glyc3P + 1 Choline> 1 Glyc3PC
63	1 G6P> 1 Inositol
64	18 AcCoA + 33 NADH + 22 ATP + 1 Glyc3P + 1 Inositol> 1 PI
65	18 AcCoA + 33 NADH + 22 ATP + 2 Glyc3P> 1 PG
66	2 PG> 1 DPG + 1 Glyc
67 68	16 AcCoA + 1 Ser + 29 NADPH + 16 ATP + 1 Choline> 2 CO2 + 1 SM 18 AcCoA + 14 NADPH + 18 ATP> 9 CO2 + 1 Cholesterol
08	
	Biomass Formation
69	160.1015 Ala + 235.2056 Glu + 70.3787 Gln + 174.6799 Gly + 114.9787 Ser +
	147.4132 Lys + 157.4070 Leu + 82.6648 Ile + 91.8543 Arg + 169.492 Asp +
	95.7754 Thr + 118.3569 Val + 40.0354 Met + 67.4027 Phe + 47.4956 Tyr + 36.2551 His + 55.559 Pro + 70.3787 Asn + 83943.063 ATP + 8.943 AMPRN +
	4.878 Cholesterol + 14.9321 CMPRN + 4.0108 dAMP + 2.6829 dCMP + 2.6829
	dGMP + 4.0108 dTMP + 0.813 DPG + 75.609 Glycogen + 16.9104 GMPRN +
	18.699 PC + 7.046 PE + 0.271 PG + 2.71 PI + 0.813 PS + 2.168 SM + 8.943
	UMPRN + 9.2297 Trp> 1 X
	Other by-products
	omer of products

70	1 AcCoA> 1 ATP + 1 Acetate
71	1 NADH + 1 DHAP> 1 Glyc3P
72	1 Glyc3P> 1 Glyc
	IgG Glycosylation
73	1 UDPG> 1 UDPGal
74	1 Glc + 3 ATP + 1 GMPRN> 1 GDPMann
75	1 AcCoA + 1 Gln + 1 F6P + 1 UMPRN + 2 ATP> 1 Glu + 1 UDPNAG
76	3 ATP + 1 3PG + 1 UDPNAG + 1 CMPRN> 1 CMPSialic
77	1 NADPH + 1 GDPMann> 1 GDPFuc
, ,	IgG Formation
78	428.7 Ala + 362.75 Glu + 351.76 Gln + 516.64 Gly + 934.36 Ser + 472.67 Lys
70	+ 516.64 Leu + 175.88 Ile + 307.79 Arg + 296.8 Asp + 626.57 Thr + 714.51 Val
	+ 65.954 Met + 285.8 Phe + 285.8 Tyr + 164.89 His + 505.65 Pro + 263.82 Asn
	+ 142.9 Trp + 10.992 GDPFuc + 54.962 UDPNAG + 32.977 GDPMann +
	21.985 UDPGal + 21.985 CMPSialic> 1 P
	Transport Reactions
79	1 ATP>
80	1 NADH>
81	1 FADH2>
82	1 NADPH>
83	1 X>
84	1 P>
85	> 1 Glc
86	> 1 His
87	1 Isobut>
88	> 1 Ile
89	1 Isoval>
90	> 1 Leu
91	> 1 Lys
92	> 1 Met
93	> 1 Phe
94	> 1 Thr
95	> 1 Trp
96	> 1 Val
97	1 CO2>
98	1 NH4>
100	1 Acetate> 1 Ala>
100	> 1 Arg
101	> 1 Arg > 1 Asn
103	> 1 Ash
103	1 Gln>
105	1 Cit>
106	> 1 Choline
107	1 Formate>
108	> 1 Glu
109	1 Glyc>
110	1 Gly>
111	1 Lac>
112	> 1 Pro
113	> 1 Pyr
114	> 1 Ser

115	> 1 Tyr
116	1 Mal>
117	1 Glyc3PC>
118	1 Glyc3PC>

Table A.2 Biomass producing Network

#	Reactions
	Glycolysis
1	1 Glc> 1 G6P
2	1 G6P> 1 F6P
3	1 F6P> 1 GAP + 1 DHAP
4	1 DHAP> 1 GAP
5	1 GAP>1 3PG
6	1 3PG> 1 Pyr
	TCA cycle
7	1 Pyr> 1 CO2 + 1 AcCoA
8	1 AcCoA + 1 Oxal> 1 Cit
9	1 Cit> 1 CO2 + 1 aKG
10	1 aKG> 1 CO2 + 1 SucCoA
11	1 SucCoA> 1 Succ
12	1 Succ> 1 Fum
13	1 Fum> 1 Mal
14	1 Mal> 1 Oxal
	Pyruvate fates
15	1 Pyr> 1 Lac
16	1 Pyr + 1 Glu> 1 Ala + 1 aKG
	Pentose Phosphate Pathway
17	3 G6P> 3 CO2 + 3 R5P
	Anaplerotic Reaction
18	1 Mal> 1 Pyr + 1 CO2
I	Amino Acid Metabolism
19	Amino Acid Metabolism
19	1 Glu <> 1 aKG + 1 NH4
20	1 Glu <> 1 aKG + 1 NH4 1 aKG + 1 Asp> 1 Glu + 1 Oxal
20 21	1 Glu <> 1 aKG + 1 NH4 1 aKG + 1 Asp> 1 Glu + 1 Oxal 1 Glu + 1 NH4> Gln
20 21 22	1 Glu <> 1 aKG + 1 NH4 1 aKG + 1 Asp> 1 Glu + 1 Oxal 1 Glu + 1 NH4> Gln 1 Thr> 1 AcCoA + 1 Gly
20 21	1 Glu <> 1 aKG + 1 NH4 1 aKG + 1 Asp> 1 Glu + 1 Oxal 1 Glu + 1 NH4> Gln 1 Thr> 1 AcCoA + 1 Gly 1 Ser> 1 Gly + 1 Formate
20 21 22 23 24	1 Glu <> 1 aKG + 1 NH4 1 aKG + 1 Asp> 1 Glu + 1 Oxal 1 Glu + 1 NH4> Gln 1 Thr> 1 AcCoA + 1 Gly 1 Ser> 1 Gly + 1 Formate 1 Ser> 1 Pyr + 1 NH4
20 21 22 23	1 Glu <> 1 aKG + 1 NH4 1 aKG + 1 Asp> 1 Glu + 1 Oxal 1 Glu + 1 NH4> Gln 1 Thr> 1 AcCoA + 1 Gly 1 Ser> 1 Gly + 1 Formate
20 21 22 23 24 25	1 Glu <> 1 aKG + 1 NH4  1 aKG + 1 Asp> 1 Glu + 1 Oxal  1 Glu + 1 NH4> Gln  1 Thr> 1 AcCoA + 1 Gly  1 Ser> 1 Gly + 1 Formate  1 Ser> 1 Pyr + 1 NH4  1 Thr> 1 NH4 + 1 aKb  1 aKb> 1 SucCoA
20 21 22 23 24 25 26	1 Glu <> 1 aKG + 1 NH4 1 aKG + 1 Asp> 1 Glu + 1 Oxal 1 Glu + 1 NH4> Gln 1 Thr> 1 AcCoA + 1 Gly 1 Ser> 1 Gly + 1 Formate 1 Ser> 1 Pyr + 1 NH4 1 Thr> 1 NH4 + 1 aKb
20 21 22 23 24 25 26 27	1 Glu <> 1 aKG + 1 NH4  1 aKG + 1 Asp> 1 Glu + 1 Oxal  1 Glu + 1 NH4> Gln  1 Thr> 1 AcCoA + 1 Gly  1 Ser> 1 Gly + 1 Formate  1 Ser> 1 Pyr + 1 NH4  1 Thr> 1 NH4 + 1 aKb  1 aKb> 1 SucCoA  1 Trp> 2 CO2 + 1 Ala + 1 aKa
20 21 22 23 24 25 26 27 28	1 Glu <> 1 aKG + 1 NH4  1 aKG + 1 Asp> 1 Glu + 1 Oxal  1 Glu + 1 NH4> Gln  1 Thr> 1 AcCoA + 1 Gly  1 Ser> 1 Gly + 1 Formate  1 Ser> 1 Pyr + 1 NH4  1 Thr> 1 NH4 + 1 aKb  1 aKb> 1 SucCoA  1 Trp> 2 CO2 + 1 Ala + 1 aKa  2 aKG + 1 Lys> 2 Glu + 1 aKa
20 21 22 23 24 25 26 27 28 29	1 Glu <> 1 aKG + 1 NH4  1 aKG + 1 Asp> 1 Glu + 1 Oxal  1 Glu + 1 NH4> Gln  1 Thr> 1 AcCoA + 1 Gly  1 Ser> 1 Gly + 1 Formate  1 Ser> 1 Pyr + 1 NH4  1 Thr> 1 NH4 + 1 aKb  1 aKb> 1 SucCoA  1 Trp> 2 CO2 + 1 Ala + 1 aKa  2 aKG + 1 Lys> 2 Glu + 1 aKa  1 aKa> 2 CO2 + 2 AcCoA
20 21 22 23 24 25 26 27 28 29 30 31 32	1 Glu <> 1 aKG + 1 NH4  1 aKG + 1 Asp> 1 Glu + 1 Oxal  1 Glu + 1 NH4> Gln  1 Thr> 1 AcCoA + 1 Gly  1 Ser> 1 Gly + 1 Formate  1 Ser> 1 Pyr + 1 NH4  1 Thr> 1 NH4 + 1 aKb  1 aKb> 1 SucCoA  1 Trp> 2 CO2 + 1 Ala + 1 aKa  2 aKG + 1 Lys> 2 Glu + 1 aKa  1 aKa> 2 CO2 + 2 AcCoA  1 aKG + 1 Val> 1 CO2 + 1 Glu + 1 IsobutCoA  1 IsobutCoA> 1 SucCoA
20 21 22 23 24 25 26 27 28 29 30 31 32 33	1 Glu <> 1 aKG + 1 NH4  1 aKG + 1 Asp> 1 Glu + 1 Oxal  1 Glu + 1 NH4> Gln  1 Thr> 1 AcCoA + 1 Gly  1 Ser> 1 Gly + 1 Formate  1 Ser> 1 Pyr + 1 NH4  1 Thr> 1 NH4 + 1 aKb  1 aKb> 1 SucCoA  1 Trp> 2 CO2 + 1 Ala + 1 aKa  2 aKG + 1 Lys> 2 Glu + 1 aKa  1 aKa> 2 CO2 + 2 AcCoA  1 aKG + 1 Val> 1 CO2 + 1 Glu + 1 IsobutCoA  1 IsobutCoA> 1 SucCoA  1 IsobutCoA> 1 Isobut  1 aKG + 1 Ile> 1 Glu + 1 AcCoA + 1 SucCoA
20 21 22 23 24 25 26 27 28 29 30 31 32	1 Glu <> 1 aKG + 1 NH4  1 aKG + 1 Asp> 1 Glu + 1 Oxal  1 Glu + 1 NH4> Gln  1 Thr> 1 AcCoA + 1 Gly  1 Ser> 1 Gly + 1 Formate  1 Ser> 1 Pyr + 1 NH4  1 Thr> 1 NH4 + 1 aKb  1 aKb> 1 SucCoA  1 Trp> 2 CO2 + 1 Ala + 1 aKa  2 aKG + 1 Lys> 2 Glu + 1 aKa  1 aKa> 2 CO2 + 2 AcCoA  1 aKG + 1 Val> 1 CO2 + 1 Glu + 1 IsobutCoA  1 IsobutCoA> 1 SucCoA
20 21 22 23 24 25 26 27 28 29 30 31 32 33 34 35	1 Glu <> 1 aKG + 1 NH4  1 aKG + 1 Asp> 1 Glu + 1 Oxal  1 Glu + 1 NH4> Gln  1 Thr> 1 AcCoA + 1 Gly  1 Ser> 1 Gly + 1 Formate  1 Ser> 1 Pyr + 1 NH4  1 Thr> 1 NH4 + 1 aKb  1 aKb> 1 SucCoA  1 Trp> 2 CO2 + 1 Ala + 1 aKa  2 aKG + 1 Lys> 2 Glu + 1 aKa  1 aKa> 2 CO2 + 2 AcCoA  1 aKG + 1 Val> 1 CO2 + 1 Glu + 1 IsobutCoA  1 IsobutCoA> 1 Isobut  1 aKG + 1 Ile> 1 Glu + 1 AcCoA + 1 SucCoA  1 aKG + 1 Leu> 1 CO2 + 1 Glu + 1 IsovalCoA  1 aKG + 1 Leu> 1 CO2 + 1 Glu + 1 IsovalCoA
20 21 22 23 24 25 26 27 28 29 30 31 32 33 34 35 36	1 Glu <> 1 aKG + 1 NH4  1 aKG + 1 Asp> 1 Glu + 1 Oxal  1 Glu + 1 NH4> Gln  1 Thr> 1 AcCoA + 1 Gly  1 Ser> 1 Gly + 1 Formate  1 Ser> 1 Pyr + 1 NH4  1 Thr> 1 NH4 + 1 aKb  1 aKb> 1 SucCoA  1 Trp> 2 CO2 + 1 Ala + 1 aKa  2 aKG + 1 Lys> 2 Glu + 1 aKa  1 aKa> 2 CO2 + 2 AcCoA  1 aKG + 1 Val> 1 CO2 + 1 Glu + 1 IsobutCoA  1 IsobutCoA> 1 Isobut  1 aKG + 1 Ile> 1 Glu + 1 AcCoA + 1 SucCoA  1 aKG + 1 Leu> 1 CO2 + 1 Glu + 1 IsovalCoA  1 aKG + 1 Leu> 1 CO2 + 1 Glu + 1 IsovalCoA
20 21 22 23 24 25 26 27 28 29 30 31 32 33 34 35 36 37	1 Glu <> 1 aKG + 1 NH4  1 aKG + 1 Asp> 1 Glu + 1 Oxal  1 Glu + 1 NH4> Gln  1 Thr> 1 AcCoA + 1 Gly  1 Ser> 1 Gly + 1 Formate  1 Ser> 1 Pyr + 1 NH4  1 Thr> 1 NH4 + 1 aKb  1 aKb> 1 SucCoA  1 Trp> 2 CO2 + 1 Ala + 1 aKa  2 aKG + 1 Lys> 2 Glu + 1 aKa  1 aKa> 2 CO2 + 2 AcCoA  1 aKG + 1 Val> 1 CO2 + 1 Glu + 1 IsobutCoA  1 IsobutCoA> 1 SucCoA  1 IsobutCoA> 1 Isobut  1 aKG + 1 Ile> 1 Glu + 1 AcCoA + 1 SucCoA  1 aKG + 1 Leu> 1 CO2 + 1 Glu + 1 IsovalCoA  1 aKG + 1 Leu> 1 SucCoA
20 21 22 23 24 25 26 27 28 29 30 31 32 33 34 35 36 37 38	1 Glu <> 1 aKG + 1 NH4  1 aKG + 1 Asp> 1 Glu + 1 Oxal  1 Glu + 1 NH4> Gln  1 Thr> 1 AcCoA + 1 Gly  1 Ser> 1 Gly + 1 Formate  1 Ser> 1 Pyr + 1 NH4  1 Thr> 1 NH4 + 1 aKb  1 aKb> 1 SucCoA  1 Trp> 2 CO2 + 1 Ala + 1 aKa  2 aKG + 1 Lys> 2 Glu + 1 aKa  1 aKa> 2 CO2 + 2 AcCoA  1 aKG + 1 Val> 1 CO2 + 1 Glu + 1 IsobutCoA  1 IsobutCoA> 1 SucCoA  1 IsobutCoA> 1 Glu + 1 AcCoA + 1 SucCoA  1 aKG + 1 Ile> 1 Glu + 1 AcCoA + 1 SucCoA  1 aKG + 1 Iso> 1 CO2 + 1 Glu + 1 IsovalCoA  1 aKG + 1 IsocCoA + 1 IsovalCoA  1 aKG + 1 IsocCoA + 1 IsovalCoA  1 CO2 + 1 SucCoA + 1 IsovalCoA  1 CO2 + 1 SucCoA + 1 IsovalCoA> 3 AcCoA + 1 SucC  1 IsovalCoA> 1 Isoval  1 Phe> 1 Tyr  1 aKG + 1 SucCoA + 1 Tyr> 1 CO2 + 1 Glu + 2 AcCoA + 1 Fum + 1 Succ
20 21 22 23 24 25 26 27 28 29 30 31 32 33 34 35 36 37 38 39	1 Glu <> 1 aKG + 1 NH4  1 aKG + 1 Asp> 1 Glu + 1 Oxal  1 Glu + 1 NH4> Gln  1 Thr> 1 AcCoA + 1 Gly  1 Ser> 1 Gly + 1 Formate  1 Ser> 1 Pyr + 1 NH4  1 Thr> 1 NH4 + 1 aKb  1 aKb> 1 SucCoA  1 Trp> 2 CO2 + 1 Ala + 1 aKa  2 aKG + 1 Lys> 2 Glu + 1 aKa  1 aKa> 2 CO2 + 2 AcCoA  1 aKG + 1 Val> 1 CO2 + 1 Glu + 1 IsobutCoA  1 IsobutCoA> 1 Isobut  1 aKG + 1 Ile> 1 Glu + 1 AcCoA + 1 SucCoA  1 aKG + 1 Leu> 1 CO2 + 1 Glu + 1 IsovalCoA  1 aKG + 1 Leu> 1 SucCoA  1 aKG + 1 Leu> 1 SucCoA  1 aKG + 1 Leu> 1 Glu + 1 AcCoA + 1 SucCoA  1 aKG + 1 Leu> 1 CO2 + 1 Glu + 1 IsovalCoA  1 CO2 + 1 SucCoA + 1 IsovalCoA  1 CO2 + 1 SucCoA + 1 IsovalCoA  1 CO2 + 1 SucCoA + 1 IsovalCoA> 3 AcCoA + 1 Succ  1 IsovalCoA> 1 Isoval  1 Phe> 1 Tyr  1 aKG + 1 SucCoA + 1 Tyr> 1 CO2 + 1 Glu + 2 AcCoA + 1 Fum + 1 Succ  1 Ser + 1 Met> 1 NH4 + 1 aKb
20 21 22 23 24 25 26 27 28 29 30 31 32 33 34 35 36 37 38 39 40	1 Glu <> 1 aKG + 1 NH4  1 aKG + 1 Asp> 1 Glu + 1 Oxal  1 Glu + 1 NH4> Gln  1 Thr> 1 AcCoA + 1 Gly  1 Ser> 1 Gly + 1 Formate  1 Ser> 1 Pyr + 1 NH4  1 Thr> 1 NH4 + 1 aKb  1 aKb> 1 SucCoA  1 Trp> 2 CO2 + 1 Ala + 1 aKa  2 aKG + 1 Lys> 2 Glu + 1 aKa  1 aKa> 2 CO2 + 2 AcCoA  1 IsobutCoA> 1 SucCoA  1 IsobutCoA> 1 Isobut  1 aKG + 1 Ile> 1 Glu + 1 AcCoA + 1 SucCoA  1 aKG + 1 Leu> 1 Glu + 1 AcCoA + 1 SucCoA  1 aKG + 1 Leu> 1 Glu + 1 AcCoA + 1 SucCoA  1 aKG + 1 Leu> 1 Glu + 1 AcCoA + 1 SucCoA  1 aKG + 1 Leu> 1 Glu + 1 AcCoA + 1 SucCoA  1 aKG + 1 Leu> 1 CO2 + 1 Glu + 1 IsovalCoA  1 cO2 + 1 SucCoA + 1 IsovalCoA> 3 AcCoA + 1 SucC  1 IsovalCoA> 1 Isoval  1 Phe> 1 Tyr  1 aKG + 1 SucCoA + 1 Tyr> 1 CO2 + 1 Glu + 2 AcCoA + 1 Fum + 1 Succ  1 Ser + 1 Met> 1 NH4 + 1 aKb  1 Asn> 1 NH4 + 1 Asp
20 21 22 23 24 25 26 27 28 29 30 31 32 33 34 35 36 37 38	1 Glu <> 1 aKG + 1 NH4  1 aKG + 1 Asp> 1 Glu + 1 Oxal  1 Glu + 1 NH4> Gln  1 Thr> 1 AcCoA + 1 Gly  1 Ser> 1 Gly + 1 Formate  1 Ser> 1 Pyr + 1 NH4  1 Thr> 1 NH4 + 1 aKb  1 aKb> 1 SucCoA  1 Trp> 2 CO2 + 1 Ala + 1 aKa  2 aKG + 1 Lys> 2 Glu + 1 aKa  1 aKa> 2 CO2 + 2 AcCoA  1 aKG + 1 Val> 1 CO2 + 1 Glu + 1 IsobutCoA  1 IsobutCoA> 1 Isobut  1 aKG + 1 Ile> 1 Glu + 1 AcCoA + 1 SucCoA  1 aKG + 1 Leu> 1 CO2 + 1 Glu + 1 IsovalCoA  1 aKG + 1 Leu> 1 SucCoA  1 aKG + 1 Leu> 1 SucCoA  1 aKG + 1 Leu> 1 Glu + 1 AcCoA + 1 SucCoA  1 aKG + 1 Leu> 1 CO2 + 1 Glu + 1 IsovalCoA  1 CO2 + 1 SucCoA + 1 IsovalCoA  1 CO2 + 1 SucCoA + 1 IsovalCoA  1 CO2 + 1 SucCoA + 1 IsovalCoA> 3 AcCoA + 1 Succ  1 IsovalCoA> 1 Isoval  1 Phe> 1 Tyr  1 aKG + 1 SucCoA + 1 Tyr> 1 CO2 + 1 Glu + 2 AcCoA + 1 Fum + 1 Succ  1 Ser + 1 Met> 1 NH4 + 1 aKb

43	1 His> 1 Glu + 1 NH4
	Glycogen Synthesis
44	1 G6P> 1 G1P
45	1 G1P + 1 UMPRN> 1 UDPG
46	1 UDPG> 1 Glycogen
	Nucleotide Synthesis
47	1 R5P> 1 PRPP
48	1 CO2 + 2 Gln + 1 Gly + 1 Asp + 1 PRPP> 2 Glu + 1 Fum + 1 IMP
49	1 Asp + 1 GMPRN + 1 IMP> 1 Fum + 1 AMPRN
50	1 Gln + 1 IMP> 1 Glu + 1 GMPRN
51	1 NH4 + 1 Asp + 1 CO2> 1 Orotate
52	1 Orotate + 1 PRPP> 1 CO2 + 1 UMPRN
53	1 Gln + 1 UMPRN> 1 Glu + 1 CMPRN
54	1 AMPRN> 1 dAMP
55	1 GMPRN> 1 dGMP
56	1 CMPRN> 1 dCMP
57	1 UMPRN> 1 dTMP
	Lipid Synthesis
58	1 Choline> 1 Pcholine
59	18 AcCoA + 1 Glyc3P + 1 Pcholine> 1 PC
60	1 Ser + 1 PC> 1 PS + 1 Choline
61	1 PS> 1 CO2 + 1 PE
62	1 Glyc3P + 1 Choline> 1 Glyc3PC
63	1 G6P> 1 Inositol
64	18 AcCoA + 1 Glyc3P + 1 Inositol> 1 PI
65	18 AcCoA + 2 Glyc3P> 1 PG
66	2 PG> 1 DPG + 1 Glyc
67	16 AcCoA + 1 Ser + 1 Choline> 2 CO2 + 1 SM
68	18 AcCoA> 9 CO2 + 1 Cholesterol
	Biomass Formation
69	160.1015 Ala + 235.2056 Glu + 70.3787 Gln + 174.6799 Gly + 114.9787 Ser + 147.4132 Lys + 157.4070 Leu + 82.6648 Ile + 91.8543 Arg + 169.492 Asp + 95.7754
	Thr + 118.3569 Val + 40.0354 Met + 67.4027 Phe + 47.4956 Tyr + 36.2551 His +
	55.559 Pro + 70.3787 Asn + 8.943 AMPRN + 4.878 Cholesterol + 14.9321 CMPRN
	+ 4.0108 dAMP + 2.6829 dCMP + 2.6829 dGMP + 4.0108 dTMP + 0.813 DPG +
	75.609 Glycogen + 16.9104 GMPRN + 18.699 PC + 7.046 PE + 0.271 PG + 2.71 PI
	+ 0.813 PS + 2.168 SM + 8.943 UMPRN + 9.2297 Trp> 1 X
	Other by-products
70	1 AcCoA> 1 Acetate
71	1 DHAP> 1 Glyc3P
72	1 Glyc3P> 1 Glyc
	Transport Reactions
73	1 X>
74	> 1 Glc
75	> 1 His
76	1 Isobut>
77	> 1 Ile
78	1 Isoval>
79	> 1 Leu
80	> 1 Lys
81	> 1 Met

0.0	1 DI
82	> 1 Phe
83	> 1 Thr
84	> 1 Trp
85	> 1 Val
86	1 CO2>
87	1 NH4>
88	1 Acetate>
89	1 Ala>
90	> 1 Arg
91	> 1 Asn
92	> 1 Asp
93	1 Gln>
94	1 Cit>
95	> 1 Choline
96	1 Formate>
97	> 1 Glu
98	1 Glyc>
99	1 Gly>
100	1 Lac>
101	> 1 Pro
102	> 1 Pyr
103	> 1 Ser
104	> 1 Tyr
105	1 Mal>
106	1 Glyc3PC>

Table A.3 Product Producing Network

#	Reactions
	Glycolysis
1	1 Glc> 1 G6P
2	1 G6P> 1 F6P
3	1 F6P> 1 GAP + 1 DHAP
4	1 DHAP> 1 GAP
5	1 GAP>1 3PG
6	1 3PG> 1 Pyr
	TCA cycle
7	1 Pyr> 1 CO2 + 1 AcCoA
8	1 AcCoA + 1 Oxal> 1 Cit
9	1 Cit> 1 CO2 + 1 aKG
10	1 aKG> 1 CO2 + 1 SucCoA
11	1 SucCoA> 1 Succ
12	1 Succ> 1 Fum
13	1 Fum> 1 Mal
14	1 Mal> 1 Oxal
	Pyruvate fates
15	1 Pyr> 1 Lac
16	1 Pyr + 1 Glu> 1 Ala + 1 aKG
	Pentose Phosphate Pathway
17	3 G6P> 3 CO2 + 3 R5P
	Anaplerotic Reaction
18	1 Mal> 1 Pyr + 1 CO2
	Amino Acid Metabolism
19	1 Glu <> 1 aKG + 1 NH4
20	$1 \text{ aKG} + 1 \text{ Asp} \longrightarrow 1 \text{ Glu} + 1 \text{ Oxal}$
21	1 Glu + 1 NH4> Gln
22	1 Thr> 1 AcCoA + 1 Gly
23	1 Ser> 1 Gly + 1 Formate
24	1 Ser> 1 Pyr + 1 NH4
25	1 Thr> 1 NH4 + 1 aKb
26	1 aKb> 1 SucCoA
27	1 Trp> 2 CO2 + 1 Ala + 1 aKa
28	2 aKG + 1 Lys> 2 Glu + 1 aKa
29	1 aKa> 2 CO2 + 2 AcCoA
30	1 aKG + 1 Val> 1 CO2 + 1 Glu + 1 IsobutCoA
31	1 IsobutCoA> 1 SucCoA
32	1 IsobutCoA> 1 Isobut
33	1 aKG + 1 Ile> 1 Glu + 1 AcCoA + 1 SucCoA
34	1 aKG + 1 Leu> 1 CO2 + 1 Glu + 1 IsovalCoA
35	1 CO2 + 1 SucCoA + 1 IsovalCoA> 3 AcCoA + 1 Succ
36	1 IsovalCoA> 1 Isoval
37	1 Phe> 1 Tyr
38	1 aKG + 1 SucCoA + 1 Tyr> 1 CO2 + 1 Glu + 2 AcCoA + 1 Fum + 1 Succ
39	1 Ser + 1 Met> 1 NH4 + 1 aKb
40	1 Asn> 1 NH4 + 1 Asp

41	1 Pro> 1 Glu		
42	1 aKG + 1 Arg> 2 Glu		
43	1 His> 1 Glu + 1 NH4		
-13	Glycogen Synthesis		
44	1 G6P> 1 G1P		
45	1 G1P + 1 UMPRN> 1 UDPG		
4	Nucleotide Synthesis		
46	1 R5P> 1 PRPP		
47	1 CO2 + 2 Gln + 1 Gly + 1 Asp + 1 PRPP> 2 Glu + 1 Fum + 1 IMP		
48	1 Gln + 1 IMP> 1 Glu + 1 GMPRN		
49	1 NH4 + 1 Asp + 1 CO2> 1 Orotate		
50	1 Orotate + 1 PRPP> 1 CO2 + 1 UMPRN		
51	1 Gln + 1 UMPRN> 1 Glu + 1 CMPRN		
	Other by-products		
52	1 AcCoA> 1 Acetate		
53	1 DHAP> 1 Glyc3P		
54	1 Glyc3P> 1 Glyc		
	IgG Glycosylation		
55	1 UDPG> 1 UDPGal		
56	1 Glc + 1 GMPRN> 1 GDPMann		
57	1 AcCoA + 1 Gln + 1 F6P + 1 UMPRN> 1 Glu + 1 UDPNAG		
58	1 3PG + 1 UDPNAG + 1 CMPRN> 1 CMPSialic		
59	1 GDPMann> 1 GDPFuc		
	IgG Formation		
60	428.7 Ala + 362.75 Glu + 351.76 Gln + 516.64 Gly + 934.36 Ser + 472.67 Lys +		
	516.64 Leu + 175.88 Ile + 307.79 Arg + 296.8 Asp + 626.57 Thr + 714.51 Val +		
	65.954 Met + 285.8 Phe + 285.8 Tyr + 164.89 His + 505.65 Pro + 263.82 Asn +		
	142.9 Trp + 10.992 GDPFuc + 54.962 UDPNAG + 32.977 GDPMann + 21.985		
	UDPGal + 21.985 CMPSialic> 1 P		
	Transport Reactions		
61	1 P>		
62	> 1 Glc		
63	> 1 His		
64	1 Isobut>		
65	> 1 Ile		
66	1 Isoval>		
67	> 1 Leu		
68	> 1 Lys		
69	> 1 Met		
70 71	> 1 Phe > 1 Thr		
72	> 1 Tm		
73	> 1 TIp		
74	1 CO2>		
75	1 NH4>		
76	1 Acetate>		
77	1 Ala>		
78	> 1 Arg		
79	> 1 Asn		
80	> 1 Asp		

82	1 Cit>
83	1 Formate>
84	> 1 Glu
85	1 Glyc>
86	1 Gly>
87	1 Lac>
88	> 1 Pro
89	> 1 Pyr
90	> 1 Ser
91	> 1 Tyr
92	1 Mal>

Appendix B - Elementary mode that uses the minimum number of metabolic reactions required to synthesize 1 unit of biomass.

<b>REACTION</b>	EM	REACTIONS
<b>NUMBER</b>	COEFF	
R1	269,67	'1 Glc> 1 G6P'
R2	33,92	'1 G6P> 1 F6P'
R3	33,92	'1 F6P> 1 GAP + 1 DHAP '
R4	0	'1 DHAP> 1 GAP'
R5	33,92	'1 GAP>1 3PG'
R6	33,92	'1 3PG> 1 Pyr '
R7	202,25	'1 Pyr> 1 CO2 + 1 AcCoA '
R8	0	'1 AcCoA + 1 Oxal> 1 Cit'
R9	0	'1 Cit> 1 CO2 + 1 aKG '
R10	136,33	'1 aKG> 1 CO2 + 1 SucCoA '
R11	0	'1 SucCoA> 1 Succ'
R12	136,33	'1 Succ> 1 Fum'
R13	332,50	'1 Fum> 1 Mal'
R14	0	'1 Mal> 1 Oxal'
R15	0	'1 Pyr> 1 Lac'
R16	164,08	'1 Pyr + 1 Glu> 1 Ala + 1 aKG'
R17	51,83	'3 G6P> 3 CO2 + 3 R5P '
R18	332,50	'1 Mal> 1 Pyr + 1 CO2'
R19	325,67	'1 Glu <> 1 aKG + 1 NH4'
R20	0	'1 aKG + 1 Asp> 1 Glu + 1 Oxal'
R21	216,83	'1 Glu + 1 NH4> Gln'
R22	225,67	'1 Thr> 1 AcCoA + 1 Gly '
R23	0	'1 Ser> 1 Gly + 1 Formate'
R24	0	'1 Ser> 1 Pyr + 1 NH4'
R25	0	'1 Thr> 1 NH4 + 1 aKb'
R26	0	'1 aKb> 1 SucCoA '
R27	0	'1 Trp> 2 CO2 + 1 Ala + 1 aKa'
R28	0	'2 aKG + 1 Lys> 2 Glu + 1 aKa'
R29	0	'1 aKa> 2 CO2 + 2 AcCoA '
R30	0	'1 aKG + 1 Val> 1 CO2 + 1 Glu + 1 IsobutCoA'
R31	0	'1 IsobutCoA> 1 SucCoA '
R32	0	'1 IsobutCoA> 1 Isobut'
R33	0	'1 aKG + 1 Ile> 1 Glu + 1 AcCoA + 1 SucCoA '
R34	0	'1 aKG + 1 Leu> 1 CO2 + 1 Glu + 1 IsovalCoA'
R35	0	'1 CO2 + 1 SucCoA + 1 IsovalCoA> 3 AcCoA + 1 Succ '
R36	0	'1 IsovalCoA> 1 Isoval'
R37	185,00	'1 Phe> 1 Tyr'
R38	136,33	'1 aKG + 1 SucCoA + 1 Tyr> 1 CO2 + 1 Glu + 2 AcCoA + 1 Fum + 1 Succ'

R39	0	'1 Ser + 1 Met> 1 NH4 + 1 aKb'
R40	0	'1 Asn> 1 NH4 + 1 Asp'
R41	0	'1 Pro> 1 Glu '
R42	217,17	'1 aKG + 1 Arg> 2 Glu '
R43	0	'1 His> 1 Glu + 1 NH4'
R44	77,50	'1 G6P> 1 G1P'
R45	77,50	'1 G1P + 1 UMPRN> 1 UDPG'
R46	77,50	'1 UDPG> 1 Glycogen'
R47	155,50	'1 R5P> 1 PRPP'
R48	46,67	'1 CO2 + 2 Gln + 1 Gly + 1 Asp + 1 PRPP> 2 Glu + 1 Fum + 1 IMP'
R49	13,25	'1 Asp + 1 GMPRN + 1 IMP> 1 Fum + 1 AMPRN'
R50	33,33	'1 Gln + 1 IMP> 1 Glu + 1 GMPRN'
R51	108,83	'1 NH4 + 1 Asp + 1 CO2> 1 Orotate'
R52	108,83	'1 Orotate + 1 PRPP> 1 CO2 + 1 UMPRN'
R53	18,08	'1 Gln + 1 UMPRN> 1 Glu + 1 CMPRN'
R54	4,08	'1 AMPRN> 1 dAMP'
R55	2,75	'1 GMPRN> 1 dGMP'
R56	2,75	'1 CMPRN> 1 dCMP'
R57	4,08	'1 UMPRN> 1 dTMP'
R58	27,25	'1 Choline> 1 Pcholine'
R59	27,25	'18 AcCoA + 1 Glyc3P + 1 Pcholine> 1 PC'
R60	8,08	'1 Ser + 1 PC> 1 PS + 1 Choline'
R61	7,25	'1 PS> 1 CO2 + 1 PE'
R62	0	'1 Glyc3P + 1 Choline> 1 Glyc3PC'
R63	2,75	'1 G6P> 1 Inositol'
R64	2,75	'18 AcCoA + 1 Glyc3P + 1 Inositol> 1 PI'
R65	1,92	'18 AcCoA + 2 Glyc3P> 1 PG'
R66	0,83	'2 PG> 1 DPG + 1 Glyc'
R67	2,25	'16 AcCoA + 1 Ser + 1 Choline> 2 CO2 + 1 SM'
R68	5,00	'18 AcCoA> 9 CO2 + 1 Cholesterol'
R69	1,00	Biomass reaction synthesis (Reaction 2)
R70	0	'1 AcCoA> 1 Acetate'
R71	33,92	'1 DHAP> 1 Glyc3P'
R72	0	'1 Glyc3P> 1 Glyc'
R73	1,00	'1 X>'
R74	269,67	'> 1 Glc'
R75	37,17	'> 1 His'
R76	0	'1 Isobut>'
R77	84,75	'> 1 Ile'
R78	0	'1 Isoval>'
R79	161,33	'> 1 Leu'
R80	151,08	'> 1 Lys'
R81	41,00	'> 1 Met'
R82	254,08	'> 1 Phe'
R83	323,83	'> 1 Thr'

R84	9,50	'> 1 Trp'
R85	121,33	'> 1 Val'
R86	972,83	'1 CO2>'
R87	0	'1 NH4>'
R88	0	'1 Acetate>'
R89	0	'1 Ala>'
R90	311,33	'> 1 Arg'
R91	72,17	'> 1 Asn'
R92	342,50	'> 1 Asp'
R93	0	1 Gln>'
R94	0	'1 Cit>'
R95	21,42	'> 1 Choline'
R96	0	'1 Formate>'
R97	232,33	'> 1 Glu'
R98	0,83	'1 Glyc>'
R99	0	'1 Gly>'
R100	0	'1 Lac>'
R101	56,92	'> 1 Pro'
R102	0	'> 1 Pyr'
R103	128,17	'> 1 Ser'
R104	0	'> 1 Tyr'
R105	0	'1 Mal>'
R106	0	'1 Glyc3PC>'

Appendix C - Standard Gibbs free energy of formation of metabolites values

METABO	LITE	GIBBS
ALANINE	C(ALA)	-366,7
GLUTAMATE( <b>GLU)</b>		-716,4
GLYCINE( <b>GLY)</b>		-379,1
SERINE(SER)		-522
LYSINE(LYS)		-303,8
LEUCINE	(LEU)	-348,2
ISOLEUCINE(ILE)		-343,9
ARGININE	E(ARG)	-229,2
ASPARTAT	TE(ASP)	-726,4
THREONIN	E(THR)	-529,3
VALINE(	(VAL)	-358,7
METHIONIN	NE(MET)	-318,8
PHENYLALAN	NINE(PHE)	-207,1
TYROSINI	E(TYR)	-370,7
HISTIDIN	E(HIS)	-179,8
PROLINE	(PRO)	-285,6
ASPARAGINE( <b>ASN)</b>		-526
TRYPTOPHAN( <b>TRP)</b>		-112
GLUCOSE( <b>GLC</b> )		-916,3
ISOBUT		-368,6
ISOVAL		-362,5
PYRUVATE( <b>PYR)</b>		-483,6
CO2		-386
CITRATE	E(CIT)	-1238
NH4		-75,7
CHOLI	NE	-31,8
GLYCEROL	(GLYC)	-493,6
ACETA	TE	-369,3
LACTATE(LAC)		-532,9
MALATE(MAL)		-887,9
FORMATE		-372,1
GLY3PC		-1334
GLUTAMINE(GLN)		-525,8
ATP		-26,2
NADH		-25,4
FADH2	52,1	
NADPH	-28	
X -3359687,065		

Appendix D - Literature data cell growth rate and metabolic rates  $^{77}$ 

(The cell growth shown in (h-1) and metabolic rates in (nmol/10<sup>6</sup> cells/h) respectively)

Growth rate	0.021
Ammonia	5.52
Acetate	-0.08
Alanine	2.72
Arginine	-2.40
Asparagine	-11.6
Aspartate	-2.60
Citrate	0.51
Choline	-0.58
Formate	2.77
Fumarate	0.02
Glucose	-60.2
Glutamate	-4.57
Glutamine	0.18
Glycerol	2.91
Glycine	1.77
Histidine	-1.17
Isobutyrate	0.27
Isoleucine	-2.02
Isovalerate	0.85
Lactate	43.3
Leucine	-3.82
Lysine	-2.22
Methionine	-0.96
Phenylalanine	-1.33
Proline	-2.71
Pyruvate	-3.07
Serine	-7.20

Appendix E - Arithmetic footprint and optimal EM for biomass and IgG producing networks.

Table E.1 Arithmetic footprint and computed formula for the biomass producing network.

Metabolites	Arithmetic Footprint (nmol/10 <sup>6</sup> cells)	Optimal EM (nmol/10 <sup>6</sup> cells)
Glc	-356,20	-263,06
Pyr	-45,18	-127,04
CO2	983,73	161,46
Cit	51,46	0
Mal	82,81	218,56
Lac	14,90	0
Glu	-56,52	-482,09
Ala	76,71	0
NH4	61,41	0
Asp	-224,78	0
Gln	21,17	176,51
Thr	-336,50	-476,06
Gly	54,55	0
Ser	-312,07	-125,01
Formate	89,06	0
Trp	-67,21	-9,23
Lys	-168,29	-147,41
Val	-164,33	-118,36
Isobut	16,06	0
Ile	-128,27	-82,66
Leu	-255,46	-317,51
Isoval	16,07	0
Phe	-128,13	-114,90
Tyr	-60,61	0
Met	-92,96	-40,04
Asn	-215,80	-404,50
Pro	-117,97	-55,56
Arg	-120,90	-91,85
His	-80,80	-36,26
Choline	-46,17	-20,87
Glyc3PC	25,30	0
Glyc	46,05	0,81
Biomass(X)	1,00	1,00
Acetate	8,98	17,02

Table E.2 Arithmetic footprint and optimal EM for the IgG producing network metabolite values in

Table E.2 Arithmetic footprint and optimal EM for the IgG producing network metabolite values in

Metabolites	Arithmetic Footprint (nmol/1mg of IgG)	Optimal EM (nmol/1mg of IgG)
Glc	-390,55	-681,53
Pyr	-88,36	0
CO2	1330,80	120,92
Cit	148,34	483,66
Mal	89,48	43,97
Lac	26,75	0
Glu	-146,05	-714,51
Ala	25,11	296,79
NH4	70,61	0
Asp	-331,43	0
Gln	29,48	0
Thr	-956,37	-1187,18
Gly	4,17	0
Ser	-1516,11	-934,36
Formate	339,65	0
Trp	-194,71	-142,90
Lys	-493,11	-472,67
Val	-850,61	-714,51
Isobut	63,20	0
Ile	-234,69	-175,88
Leu	-647,85	-516,64
Isoval	63,20	0
Phe	-477,51	-428,70
Tyr	-191,71	-142,90
Met	-170,62	-65,95
Asn	-576,30	-1209,17
Pro	-651,70	-505,65
Arg	-377,61	-307,79
His	-270,76	-164,89
Acetate	261,76	0
Glyc	55,17	0
P	1,00	1,00

## Appendix F – Results from the IgG producing network footprintome automatic reduction

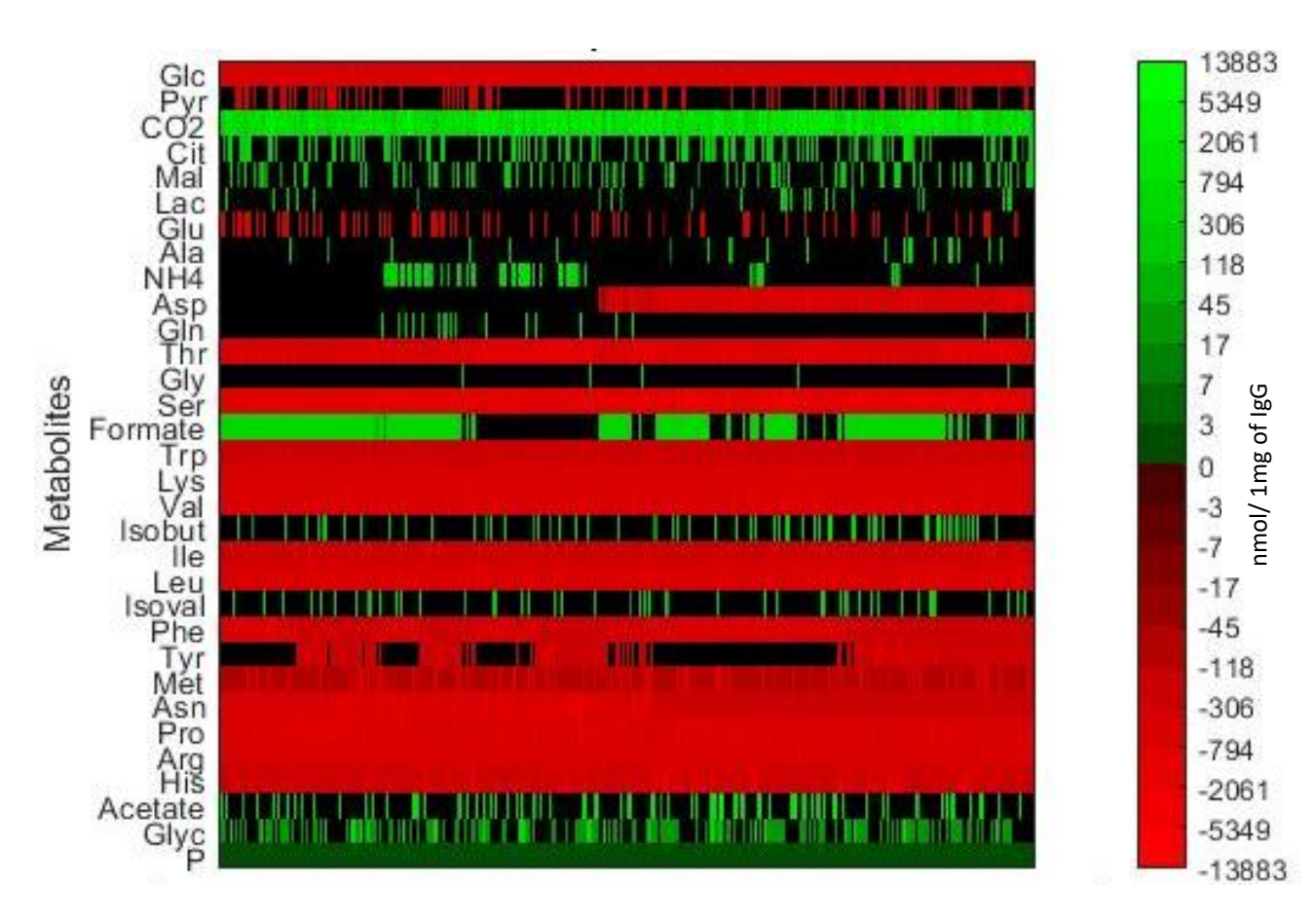


Figure F.1 Reduced *footprintome* for IgG(P) production (normalized to unit) after 2 steps of reduction: Step 1- IgG(P) production, Step 2-thermodynamic reduction. The columns represent the reduced set of EMs (307402). The colour green means that the compound is being produced by the EM. The colour red means it's being consumed by the EM. The black means it is neither consumed nor produced by the EM.

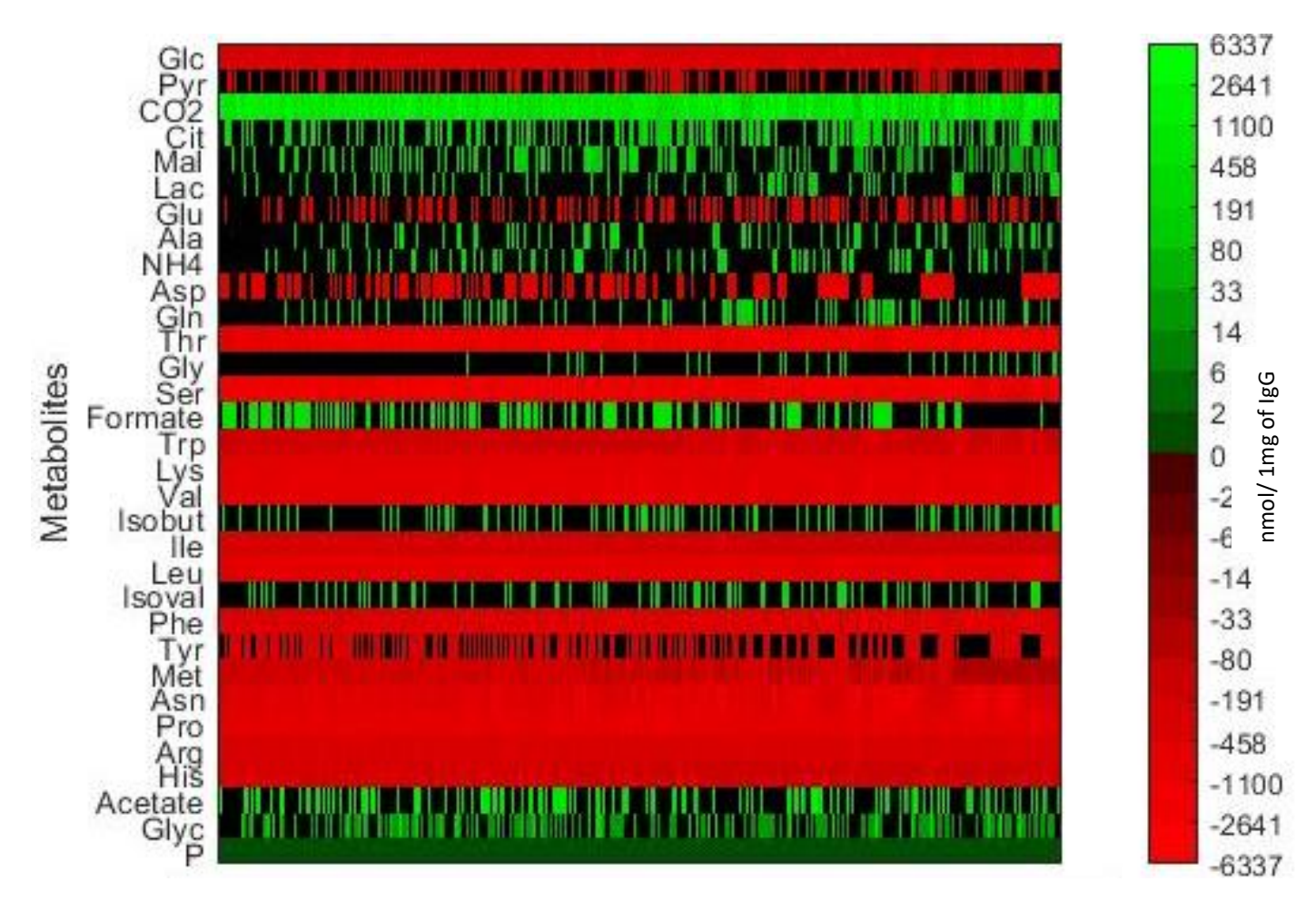


Figure F.2 Reduced footprintome for IgG (P) production (normalized to unit) after 3 steps of reduction: Step 1- IgG(P) production, Step 2-Thermodynamic reduction, Step 3- Pattern clustering with arithmetic averaging. The rows represent extracellular media components. The columns represent average EM clusters (4704). The green gradient represents compound production associated with the production of 1 biomass unit. The red gradient represents compound consumption to generate 1 IgG unit. The black colour means that the compound is neither consumed nor produced by the EM cluster.